Received: 13 December 2021 | Revised: 23 April 2022 | Accepted: 16 May 2022

DOI: 10.1002/jev2.12238

RESEARCH ARTICLE

Identification of storage conditions stabilizing extracellular vesicles preparations

André Görgens[1,2,3] | Giulia Corso[1] | Daniel W. Hagey[1] | Rim Jawad Wiklander[1] | Manuela O. Gustafsson[1] | Ulrika Felldin[1] | Yi Lee[1] | R. Beklem Bostancioglu[1] | Helena Sork[1,4] | Xiuming Liang[1] | Wenyi Zheng[1] | Dara K. Mohammad[1,5] | Simonides I. van de Wakker[6] | Pieter Vader[6,7] | Antje M. Zickler[1] | Doste R. Mamand[1] | Li Ma[8] | Margaret N. Holme[8] | Molly M. Stevens[8,9] | Oscar P. B. Wiklander[1,3] | Samir EL Andaloussi[1,3,10]

[1]Department of Laboratory Medicine, Clinical Research Center, Karolinska Institutet, Stockholm, Sweden

[2]Institute for Transfusion Medicine, University Hospital Essen, University of Duisburg-Essen, Essen, Germany

[3]Evox Therapeutics Limited, Oxford, UK

[4]Institute of Technology, University of Tartu, Tartu, Estonia

[5]College of Agricultural Engineering Sciences, Salahaddin University-Erbil, Erbil, Kurdistan Region, Iraq

[6]Department of Cardiology, Experimental Cardiology Laboratory, University Medical Center Utrecht, Utrecht University, Utrecht, The Netherlands

[7]CDL Research, University Medical Center Utrecht, Utrecht University, Utrecht, The Netherlands

[8]Department of Medical Biochemistry and Biophysics, Karolinska Institutet, Stockholm, Sweden

[9]Department of Materials, Department of Bioengineering, and Institute of Biomedical Engineering, Imperial College London, London, UK

[10]Department of Physiology, Anatomy and Genetics, University of Oxford, Oxford, UK

Correspondence
André Görgens and Samir EL Andaloussi, Department of Laboratory Medicine, Clinical Research Center, Karolinska Institutet, Stockholm, Sweden.
Email: andre.gorgens@ki.se, and samir.el-andaloussi@ki.se

Funding information
H2020 (EXPERT); Evox Therapeutics; Mobilitas Pluss (MOBJD512); KI Research grant; SSF-IRC (FormulaEx); Center for Medical Innovation (CIMED); ISAC Marylou Ingram Scholarship; The European Regional Development Fund; H2020 European Research Council, Grant/Award Number: 4-628/2021; Vetenskapsrådet, Grant/Award Number: 4-258/2021

Abstract

Extracellular vesicles (EVs) play a key role in many physiological and pathophysiological processes and hold great potential for therapeutic and diagnostic use. Despite significant advances within the last decade, the key issue of EV storage stability remains unresolved and under investigated. Here, we aimed to identify storage conditions stabilizing EVs and comprehensively compared the impact of various storage buffer formulations at different temperatures on EVs derived from different cellular sources for up to 2 years. EV features including concentration, diameter, surface protein profile and nucleic acid contents were assessed by complementary methods, and engineered EVs containing fluorophores or functionalized surface proteins were utilized to compare cellular uptake and ligand binding. We show that storing EVs in PBS over time leads to drastically reduced recovery particularly for pure EV samples at all temperatures tested, starting already within days. We further report that using PBS as diluent was found to result in severely reduced EV recovery rates already within minutes. Several of the tested new buffer conditions largely prevented the observed effects, the lead candidate being PBS supplemented with human albumin and trehalose (PBS-HAT). We report that PBS-HAT buffer facilitates clearly improved short-term and

long-term EV preservation for samples stored at -80°C, stability throughout several freeze-thaw cycles, and drastically improved EV recovery when using a diluent for EV samples for downstream applications.

KEYWORDS
diluent, exosomes, extracellular vesicles, liposomes, preservation, stability, storage, storage buffer, vesicles

1 | INTRODUCTION

Within the last decade, various aspects of extracellular vesicles (EVs) have been investigated in numerous studies addressing their basic biology, their role in various physiological and pathophysiological processes, and their promising potential for clinical use in context of therapy and diagnostics (Lener et al., 2015; Lotvall et al., 2014; Mateescu et al., 2017; Sahoo et al., 2021; Weng et al., 2021; Wiklander et al., 2019; Yanez-Mo et al., 2015). Despite ongoing efforts and advances to improve standardization of data reporting and procedures related to EV isolation and characterization in the field, lots of open questions and challenges remain (Coumans et al., 2017; Ramirez et al., 2018; Thery et al., 2018; Welsh et al., 2020; Welsh et al., 2021). Particularly our knowledge about the impact of storage conditions on EVs is still scarce, and the field lacks defined and standardized conditions for EV preservation even though storage stability is a key issue and a prerequisite to facilitate stability of bio-banked clinical samples and production of consistent EV batches for therapeutic use (Thery et al., 2018; Witwer et al., 2013; Yuan et al., 2021).

Effects of storage conditions on EVs have been investigated in a number of studies so far, demonstrating that storage related factors may affect various EV characteristics including biophysical stability, particle recovery and diameter, and function of EVs (Bosch et al., 2016; Coumans et al., 2017; Jeyaram & Jay, 2017; Kusuma et al., 2018; Lener et al., 2015; Lőrincz et al., 2014; Maroto et al., 2017; Mateescu et al., 2017; Sokolova et al., 2011; Yuana et al., 2015; Zhou et al., 2006). Phosphate-buffered saline (PBS) so far has been the preferred storage buffer in a majority of studies and concluding recommendations have been to store aliquots at -80°C (Kusuma et al., 2018; Witwer et al., 2013). A few studies in the last years have investigated the impact of storage temperature and time (Cheng et al., 2019; Lőrincz et al., 2014; Park et al., 2018), focused on the role of plastic tubes used for isolation or storage (Evtushenko et al., 2021; Resnik et al., 2020), or explored the use of cryoprotective additives such as DMSO (Tegegn et al., 2016) or trehalose (Bosch et al., 2016). More recent comprehensive studies investigated EV stability in context of lyophilisation (Trenkenschuh et al., 2022), storage-related particle loss through vesicle fusion (Gelibter et al., 2022), and the short-term influence of storage conditions and concentration methods on EV recovery and function (van de Wakker et al., 2021). Generally, reported findings have sometimes been conflicting, likely related to a focus on storage procedures for specific biofluid samples, to specific storage strategies in terms of EV isolation procedures, or to limited downstream read-outs only covering partial aspects of EVs such as small RNA quantification or bulk protein content in several studies (Jeyaram & Jay, 2017; Kusuma et al., 2018; Qin et al., 2020; Welch et al., 2017; Yuan et al., 2021). This is particularly relevant since the EV source and choice of isolation method is known to affect EV composition, recovery, and purity (Allelein et al., 2021; Nordin et al., 2015; Willms et al., 2018). To date, there is still a lack of consensus concerning the impact of storage conditions on EVs, and more comprehensive studies systematically comparing different storage strategies over longer timeframes are needed in order to identify storage conditions stabilizing extracellular vesicle preparations, especially for purified EV samples derived from cell culture supernatants.

Aiming to identify conditions for long-term storage of EVs, we here share a detailed dataset summarizing efforts to further understand EV stability over time in our labs. We included EVs isolated through different isolation procedures from the cell culture supernatant of different cellular sources and set up a study evaluating different EV preservation strategies for up to 2 years. Following storage of EV samples in different buffers and at different temperatures, samples were analysed over time by various methods including Nanoparticle Tracking Analysis (NTA), bead-based multiplex flow cytometry, and single vesicle imaging flow cytometry (IFCM). In addition, different EV engineering strategies were employed to utilize specifically introduced modifications for assessing further parameters such as cellular uptake, ligand binding, and fluorescence stability of intravesicular proteins. The results presented here altogether contribute to identifying improved buffers for EV preservation and handling and improve our understanding of how storage conditions affect EV quality and recovery.

2 | MATERIAL AND METHODS

2.1 | Cells and cell culture

HEK293T (human embryonic kidney-293T) cells were cultured in Dulbecco's modified Eagle's medium (DMEM) containing Glutamax-I and sodium pyruvate; 4.5 g/L Glucose; Invitrogen) supplemented with 10% foetal bovine serum (FBS; Invitrogen)

and 1% Antibiotic-Antimycotic (Anti-Anti; ThermoFisher Scientific). Immortalized human bone marrow-derived mesenchymal stromal cells (MSCs) (Mihara et al., 2003) were cultured in Roswell Park Memorial Institute (RPMI-1640) medium containing Glutamax-I and 25 mM HEPES (Invitrogen) supplemented with 10% FBS (Invitrogen), 10^{-6} mol/L hydrocortisone (Sigma) and 1% Anti-Anti. 48 h prior to collection of conditioned media for EV isolation from HEK293T cells or MSCs, cells were washed with PBS and the medium was changed to OptiMem (Invitrogen). HEK293 Freestyle suspension cells (HEK293FS; ThermoFisher Scientific) were cultured in FreeStyle 293 Expression Medium (ThermoFisher Scientific) in 125 ml polycarbonate Erlenmeyer flasks (Corning) in a shaking incubator (Infors HT Minitron) according to the manufacturer's instructions. All cell lines were grown at 37°C, 5% CO_2 in a humidified atmosphere and regularly tested for the presence of mycoplasma. The creation and characterization of the genetically modified stable cell lines HEK293T:CD63eGFP (Corso et al., 2017), HEK293T:CD63mNG (Wiklander et al., 2018), HEK293FS:CD63mNG (HEK293 FreeStyle:CD63mNeonGreen) (Cavallaro et al., 2021), and MSC:TNFR1 (Gupta et al., 2021) were described previously.

2.2 | Isolation of EVs

Generally, cell culture-derived conditioned media (CM) was firstly pre-cleared from cells and debris by a low-speed centrifugation step (700 *x g* for 5 min) and subsequent centrifugation at 2000 *x g* for 20 min to remove larger particles and debris. Pre-cleared cell culture supernatant was subsequently filtered through 0.22 μm bottle top vacuum filters (Corning, cellulose acetate, low protein binding) to remove any larger particles.

For experiments shown in Figure 1 (Stage 1), HEK293T:CD63eGFP EVs were isolated by differential ultracentrifugation (UC) or tangential flow filtration (TFF) followed by size exclusion chromatography (SEC) as comparison. To purify EVs by UC, the pre-cleared CM was centrifuged at 100,000 *x g* for 90 min, the EV pellet was washed with 25 ml of PBS, re-pelleted at 100,000 *x g* for 90 min and resuspended in 100 μl PBS. The centrifugation steps were performed at 4°C using the Beckman Coulter Type 70 Ti rotor in a Beckman Coulter L-80 ultracentrifuge. For the TFF-SEC EV isolation, pre-cleared CM was concentrated via TFF by using the KR2i TFF system (SpectrumLabs) equipped with modified polyethersulfone (mPES) hollow fiber filters with 300 kDa membrane pore size (MidiKros, 370 cm^2 surface area, SpectrumLabs) at a flow rate of 100 ml/min (transmembrane pressure at 3.0 psi and shear rate at 3700 s^{-1}) as described previously (Corso et al., 2017; Nordin et al., 2019). The sample was then loaded on a qEV column (Izon Science) and the EV fractions (fractions 7 to 11, corresponding to ~3 ml) were collected according to the manufacturer's instructions. Amicon Ultra-0.5 10 kDa MWCO spin-filters (Millipore) were used to concentrate the sample to a final volume of 100 μl.

For experiments shown in Figure 2 (Stage 2), MSC and HEK293T:CD63eGFP derived pre-cleared CM were subjected to TFF as described above and then further concentrated through Amicon Ultra-15 10 kDa molecular weight cut-off spin-filters (Millipore).

For experiments shown in Figures 3–11 (Stage 3), EVs were additionally purified via bind-elute size exclusion chromatography (BE-SEC): CM were concentrated by TFF as described above and then loaded onto BE-SEC columns (HiScreen Capto Core 700 column, GE Healthcare Life Sciences), connected to an ÄKTAstart chromatography system (GE Healthcare Life Sciences) as described previously (Corso et al., 2017). EV samples were collected according to the 280 nm UV absorbance chromatogram and concentrated to a final volume of 500 μL by using Amicon Ultra-15 10 kDa molecular weight cut-off spin-filters (Millipore). All isolated EV samples, regardless of the purification method, were resuspended in the respective buffers, aliquoted and analysed fresh or stored at +4°C, -20°C or -80°C. Buffers were prepared by using the base buffers or cell culture media with different additives as listed in Table 1, that is, PBS (Dulbecco's PBS, cat 14190136, ThermoFisher), 0.9% NaCl (sodium chloride; injection solution, Braun), HBSS (Hanks' Balanced Salt Solution, cat 14175129, ThermoFisher), RPMI1640 (cat 72400054, ThermoFisher), 10% glucose (injection solution, Braun), IMDM (Iscove's Modified Dulbecco's Medium; cat 21980065, ThermoFisher), trehalose [D-(+)-Trehalose dihydrate, cat T0167-25G, Sigma-Aldrich], HEPES (cat 15630-080, ThermoFisher), human serum albumin (HSA, albunorm injection solution, Octapharma AB), DMSO (cat D4540, Sigma Aldrich), and glycerol (cat G5516, SigmaAldrich). All buffers were filtered through 0.22 μm filters before usage. Unless indicated otherwise, EVs were stored in Maxymum Recovery polypropylene 1.5 ml tubes (Axygen Maxymum Recovery, Corning, cat MCT-150-L-C). For tube comparison experiments (Figure 14), EVs were additionally stored in high performance USP Class VI 1.5 ml polypropylene tubes (VWR, cat 525–1164), DNA LoBind 1.5 ml tubes (Eppendorf, cat 022431021), low protein binding 1.5 ml tubes (ThermoFisher Scientific, cat 90410), 8 ml glass tubes (Qiagen) and 8 ml glass tubes coated with Sigmacote® (Sigma, cat SL2-100ML) according to the manufacturer's protocol.

2.3 | Formulation of fluorescently labelled liposomes

A lipid film composed of 1,2-dioleoyl-sn-glycero-3-phosphocholine (DOPC) (Avanti Polar Lipids), 1,2-dioleoyl-sn-glycero-3-phosphoethanolamine (DOPE) (Avanti Polar Lipids) and cholesterol (Sigma Aldrich) with a mass ratio of 50:25:25 (total mass 1.25 mg) and 2 mol% additional 1,1′-Dioctadecyl-3,3,3′,3′-Tetramethylindodicarbocyanine Perchlorate (DiD') (Invitrogen,

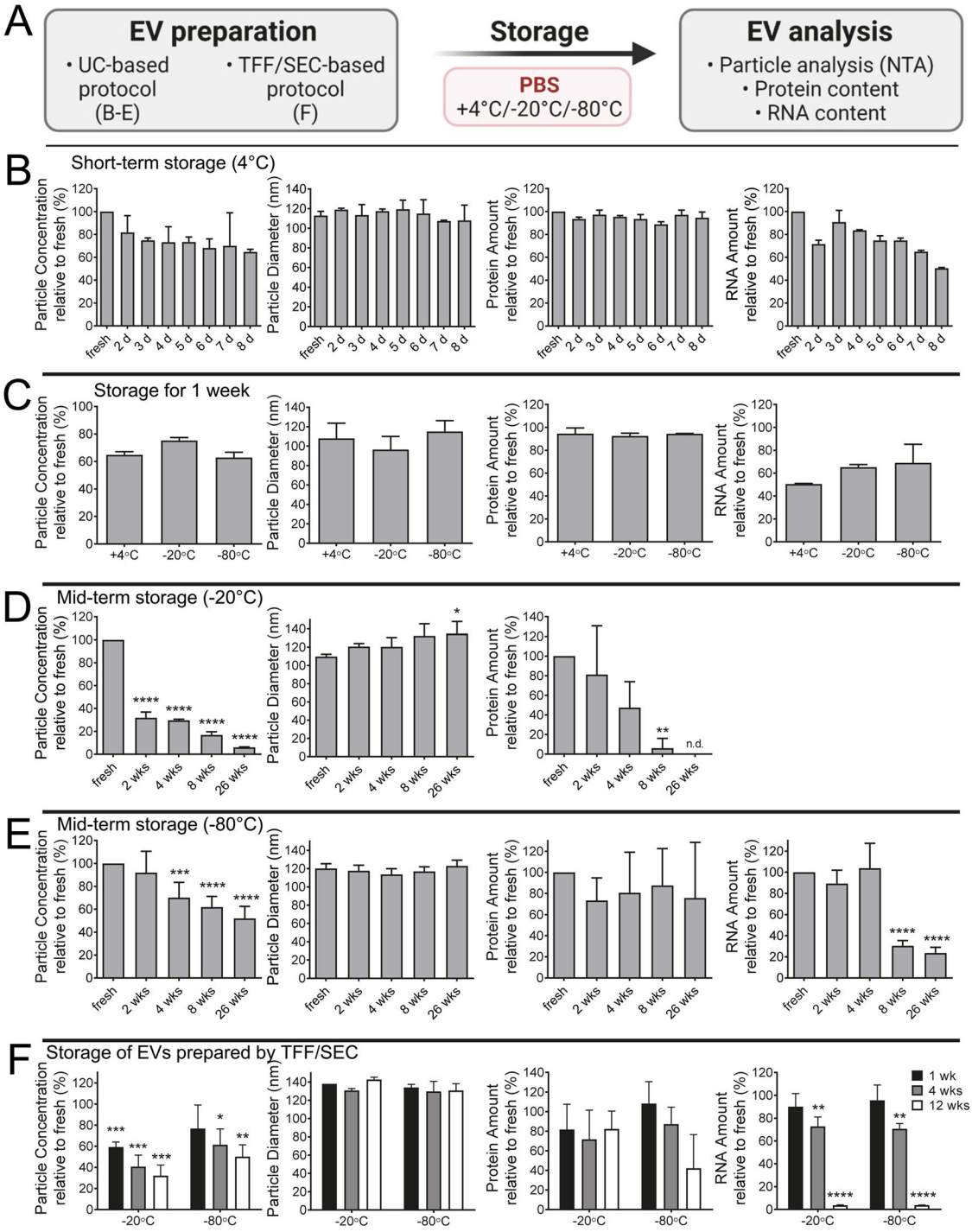

FIGURE 1 **EVs appear unstable when stored in PBS**. (A) HEK293T EVs were isolated by UC (A-E) or UF/SEC (F), and aliquots were stored in PBS at +4˚C, -20˚C or -80˚C and analysed at different time points. (B) Particle concentration and diameter estimated by NTA measurement of samples stored at +4˚C in PBS up to 8 days and estimated bulk protein amount and RNA quantifications from same sample volumes. Measurements were done daily up to 8 days ($n = 2$). Values are expressed relative to fresh samples. (C) Particle concentration and diameter estimated by NTA measurement of samples stored at +4˚C, -20˚C or -80˚C for 1 week in PBS. Estimated bulk protein amount and RNA quantifications from same sample volumes ($n = 2$). (D) NTA and protein concentration measurements from EVs stored at -20˚C in PBS for up to 26 weeks ($n = 3$; RNA data not available). (E) Results from EVs stored at -80˚C in PBS for up to 26 weeks ($n = 6$). (F) Results from TFF/SEC-purified EVs stored at -20˚C or -80˚C in PBS for 1 week, 4 weeks or 12 weeks ($n = 3$). Statistical significance was assessed by one-way ANOVA followed by Dunnet's posthoc tests. All p-values are referring to fresh values (*:$P < 0.05$; **: $P < 0.01$; ***: $P < 0.001$; ****: $P < 0.0001$; mean±SD; d: days; wks: weeks; n.d.: not detected))

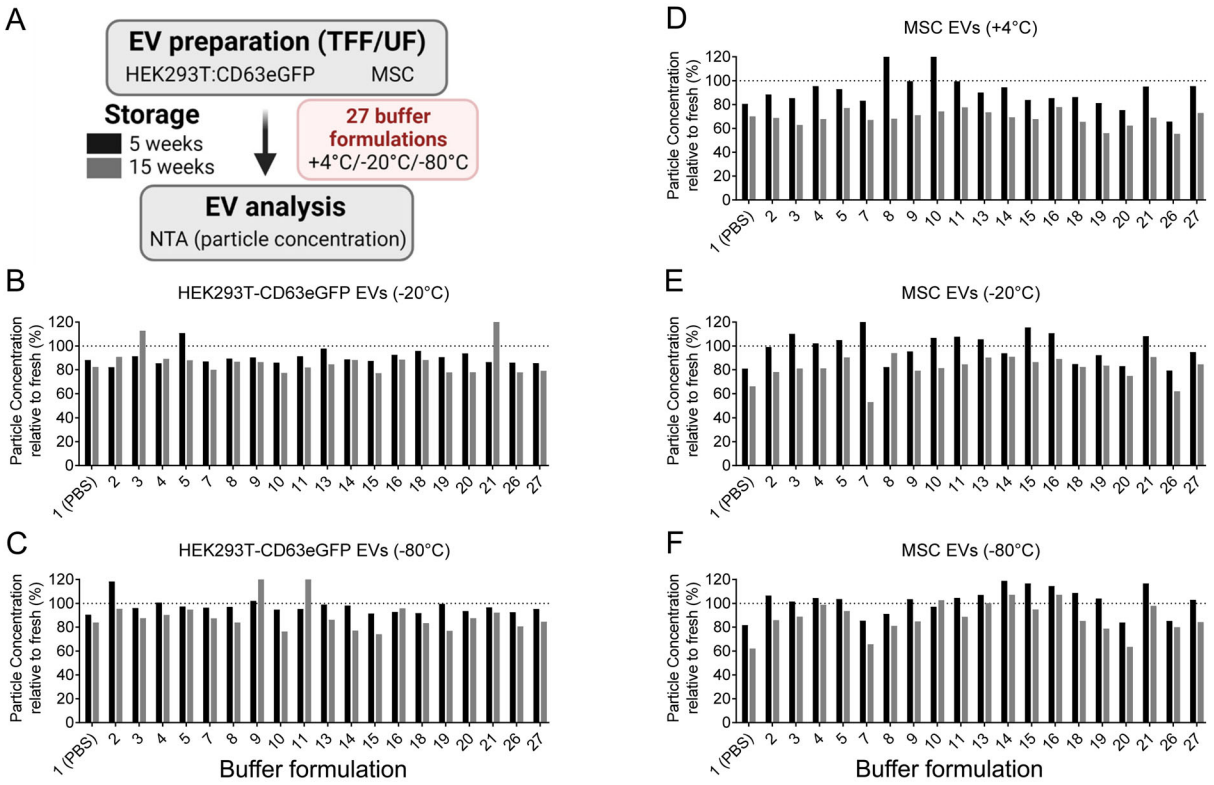

FIGURE 2 **Sample concentrations measured by NTA after EV storage in different candidate buffers**. (A) EVs were enriched from MSC or HEK293T:CD63eGFP conditioned medium by TFF/UF, diluted 10x in different buffer formulations and stored at +4˚C, -20˚C or -80˚C. NTA particle counts were measured as surrogate read-out for EV stability freshly and after 5 and 15 weeks of storage. NTA-based concentrations are provided for HEK293T:CD63eGFP EVs stored at -20˚C (B) and -80˚C (C). Most HEK293T:CD63eGFP EV aliquots stored at +4˚C showed signs of contamination and were excluded from the analysis (not shown). (D-F) Particle concentrations for MSC EVs stored at +4˚C (D), -20˚C (E) and -80˚C (F)

Thermo Fisher Scientific) was prepared via evaporation from a chloroform solution in a glass vial. After being thoroughly dried by lyophilisation (Labconco), it was rehydrated (1.25 mg/ml) in TE buffer (pH 8.0) containing 10 mM Tris-HCl (Sigma-Aldrich), 1 mM EDTA (Sigma-Aldrich) and 150 mM NaCl (Sigma-Aldrich) at 37 ˚C for 1 h. After being fully resuspended by vortex, the emulsion was extruded 31 times through a 100 nm polycarbonate membrane (Whatman) at 37 ˚C using an Avanti MiniExtruder (Avanti Polar Lipids). The liposome suspension was stored in a low adsorption glass vial (Supelco, Sigma-Aldrich) at 4 ˚C protected from light, until use.

2.4 | Nanoparticle tracking analysis

Nanoparticle tracking analysis (NTA) (Dragovic et al., 2011; Sokolova et al., 2011) was applied to determine particle size and concentration of all samples using the NanoSight NS500 instrument equipped with NTA 2.3 analytical software and an additional 488 nm laser. The samples were diluted in 0.22 μm filtered PBS to an appropriate concentration before being analysed. At least five 30 s videos were recorded per sample in light scatter mode with a camera level of 11–13. Software settings were kept constant for all EV measurements (screen gain 10, detection threshold 7). The analysis was performed with the screen gain at 10 and detection threshold at 7 for all EV measurements. Liposomes were captured at a camera level of 13 and analysed with a detection threshold of 2 (screen gain 20; Figure S13B).

2.5 | Protein quantification and RNA analysis

Protein concentration in EV samples was measured using the DC protein assay kit (Bio-Rad). RNA concentration for samples analysed in Stage 1 (Figure 1) was quantified using the Quant-iT RiboGreen RNA assay kit (Thermo Fisher Scientific). Both assays were performed according to the manufacturer's instructions. For RNA quantifications from HEK293T:CD63mNG

A

Buffer	Stage 2 no.	Base buffer	HEPES	Albumin	Trehalose	DMSO
PBS	1	PBS				
PBS-HA		PBS	+	+		
PBS-A	2	PBS		+		
PBS-AT	3	PBS		+	+	
PBS-HAT	4	PBS	+	+	+	
PBS-HATD	5	PBS	+	+	+	+
NaCl-HA		0.9% NaCl	+	+		
NaCl-HAT	10	0.9% NaCl	+	+	+	
ExoCap		ExoCap Storage Booster (commercial buffer)				

B

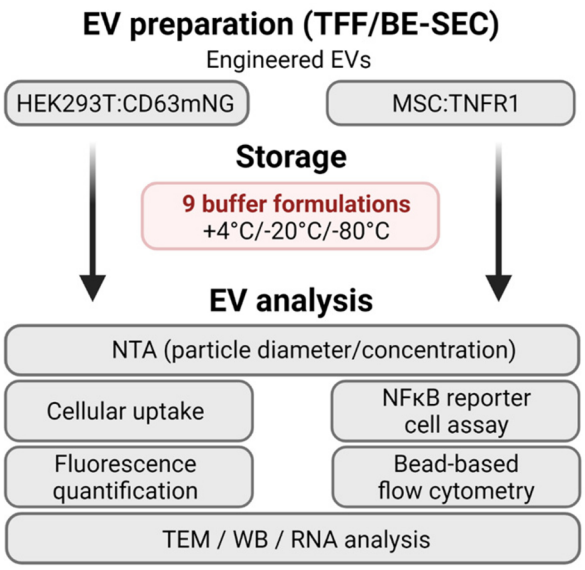

FIGURE 3 **Stage 3 candidate buffer formulation overview and experimental outline**. (A) Candidate storage buffer formulations, including PBS and Buffers 2, 3, 4, 5, and 10 from Stage 2 as well as two new variations (PBS-HA and NaCl-HA) and the commercial buffer 'Exocap Storage Booster' (ExoCap). Additives were added at the same concentrations as for Stage 2 (HSA 0.2 %; Trehalose 25 mM; HEPES 25 mM; DMSO 1%). (B) Summary of experimental outline for Stage 3

derived EVs stored for 20 weeks shown in Figure 8, RNA species in the range from 5 to 200 bp were measured on the Agilent 2100 Bioanalyzer using the smallRNA kit. For preparation of RNA for experiments shown in Figure 12, Trizol LS (Thermo Scientific) was added to EV samples. Samples were kept at -80˚C, then they were thawed and total RNA was extracted using the Direct-zol RNA microprep kit (Zymo Research) according to the manufacturer's instructions. The RNA integrity was tested on the Agilent 2100 Bioanalyzer using the smallRNA and High Sensitivity DNA kits (Agilent Technologies). RNA and cDNA concentrations were calculated using the Bioanalyzer software. For small RNAs this was calculated for all lengths spanning the chip (5-200 bp), while for full length cDNA this was calculated for all fragments between 400–10,000 bp. To judge mRNA stability, the ratio of full-length cDNA was compared to the concentration of DNA fragments < 400 bp.

To evaluate potential effects of storage buffer on cells (see Figure S4), human fibroblast cultures (GM08402; Coriell cat. GM08402, RRID:CVCL_7485) were treated with PBS-HAT buffer alone or 1×10^9 HEK293T-derived EVs in PBS-HAT buffer for 20 h. Cells were harvested, cDNA from bulk RNA was prepared for sequencing using the Smart-seq2 protocol as described previously (Hagey et al., 2020), and single end 50 bp sequencing of samples was carried out on an Illumina HiSeq3000 machine. Reads per million, per kilobase gene were calculated and the most variable genes were used to map and cluster samples using a t-distributed stochastic neighbour embedding-nearest neighbour method (Hagey et al., 2020) and hierarchical clustering in R. Differential expression between triplicate samples was performed using the Deseq2 package in R.

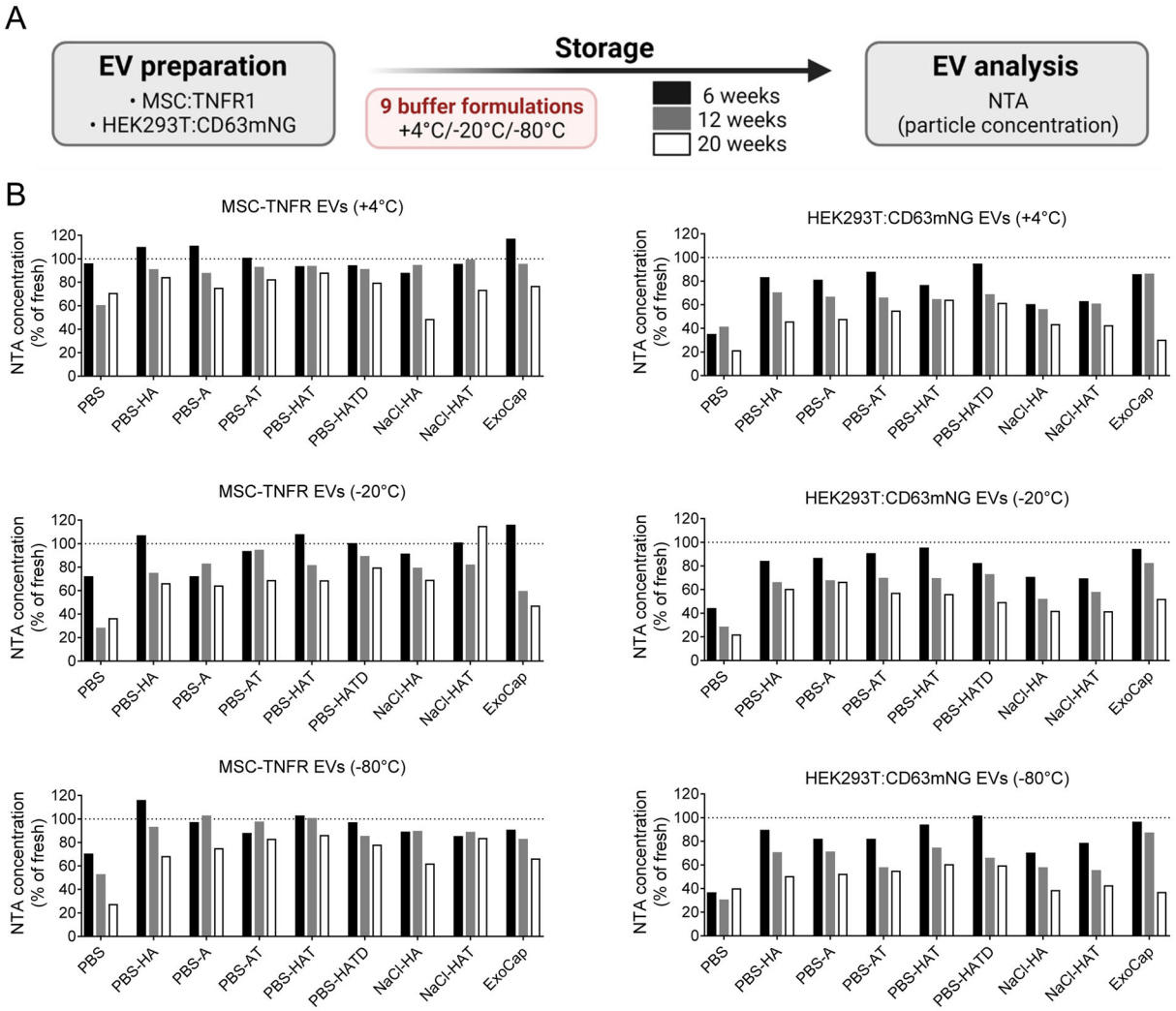

FIGURE 4 **Sample concentrations measured by NTA after EV storage in different candidate Stage 3 buffers**. (A) Engineered EVs were isolated from MSC:TNFR1 or HEK293T:CD63mNG conditioned medium by TFF/UF and subsequent BE-SEC, diluted 10x in nine different buffer formulations and stored at +4˚C, -20˚C or -80˚C. (B) NTA particle concentrations measured freshly (dotted line) and after 6, 12 and 20 weeks of storage

2.6 | Fluorescence quantification

Bulk quantification of EV fluorescence intensity (RFU) from equal volumes of CD63-mNG labelled EVs was measured using the SpectraMax i3x microplate reader (Molecular Devices). The fluorescence signal was detected from the top in an endpoint assay with excitation set at 488 nm and emission at 510 nm.

2.7 | Multiplex bead-based flow cytometry

For quantification of EV surface marker expression, EVs were subjected to multiplex bead-based flow cytometry analysis (MACSPlex Exosome Kit, human, Miltenyi Biotec) as described previously (Wiklander et al., 2018). In brief, equal amounts of volume from stored EV aliquots were loaded onto wells of a pre-wet and drained MACSPlex 96 well 0.22 μm filter plate before 8 μl of MACSPlex Exosome Capture Beads (containing 39 different antibody-coated bead subsets) were added to each well. Filter plates were then incubated on an orbital shaker overnight (14–16 h) at 450 rpm at room temperature, protected from light. The beads were washed with 200 μl of buffer and the liquid was removed by applying vacuum (Sigma-Aldrich, Supelco PlatePrep; -100 mBar). For counterstaining of EVs bound by capture beads with detection antibodies, a mixture of APC-conjugated anti-CD9, anti-CD63 and anti-CD81 detection antibodies (supplied in the kit; 5 μl each) was added to each well and the plate was incubated for 1 h at room temperature protected from light. Next, the samples were washed twice, resuspended in MACSPlex

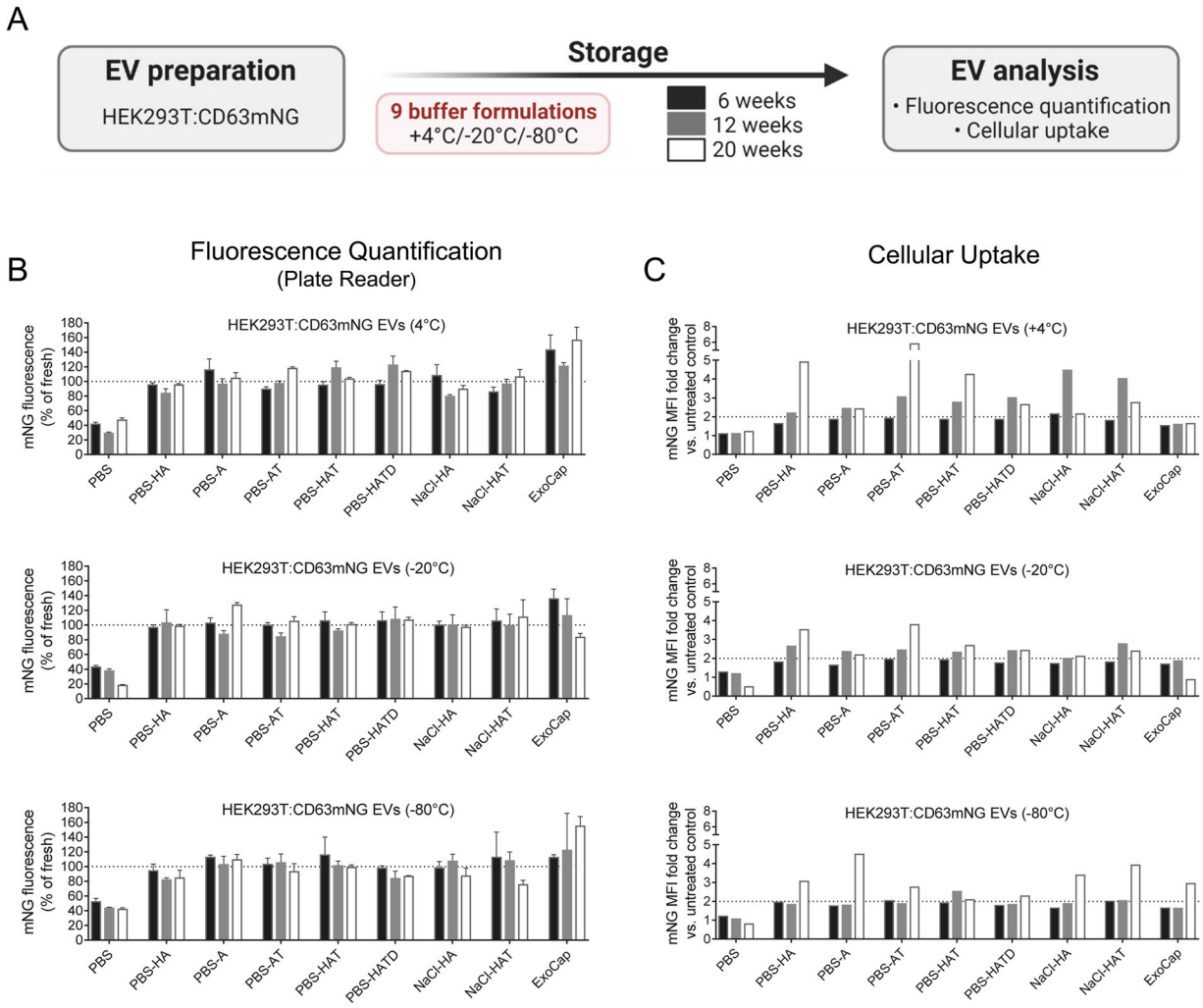

FIGURE 5 **Using fluorescence-tagged EVs to evaluate stability in various buffers.** (A) HEK293T:CD63mNG engineered fluorescent EVs were stored in respective buffers for 6, 12, and 20 weeks at +4˚C, -20˚C or -80˚C. Equal volumes from aliquots were subjected to bulk fluorescence measurements (B; $n = 2$; mean±SD) or cellular uptake assays (C; dotted line indicates fold change values obtained for fresh samples)

Buffer buffer and transferred to V-bottom 96 well microtiter plates (ThermoFisher Scientific). Flow cytometric analysis was performed with a MACSQuant Analyzer 10 flow cytometer (Miltenyi Biotec) by using the built-in 96 well plate reader. All samples were automatically mixed immediately before being loaded in the system and acquired by the instrument. FlowJo software (v10, FlowJo LLC) was used to analyse flow cytometric data. Median fluorescence intensities (MFI) for all 39 capture bead subsets were background-corrected by subtracting respective MFI values from matched non-EV buffer or media controls that were treated exactly like EV-containing samples (buffer/medium + capture beads + antibodies).

2.8 | Quantification of cellular uptake

For quantification of cellular uptake of EVs, equal volumes of HEK293T:CD63mNG engineered fluorescent EVs from each stored aliquot were added to human hepatocellular carcinoma cells (Huh-7) seeded the day before at a density of 2.5×10^4 cells per well in a 96-well plate. Cells were incubated for 2 h at 37°C, 5% CO_2 atmosphere. Temperature controls (incubation at 4°C) were not included in this study due to limited availability of samples, but were regularly performed without resulting in positive signals above background in previous studies involving the same EV source, dose and uptake protocol (Corso et al., 2017; Corso et al., 2019). After incubation, the cells were washed twice with PBS, trypsinised, spun down at 900 *x g* for 5 min and resuspended in 100 μL of PBS (Invitrogen) supplemented with 1 mM EDTA and 2% FBS. Dead cells were excluded from analysis via 4′,6-diamidino-2-phenylindole (DAPI) staining and doublets were excluded by forward/side scatter area versus height gating as described before (Corso et al., 2017; Corso et al., 2019). Samples were kept on ice and data was acquired at a MACSQuant Analyser 10 instrument.

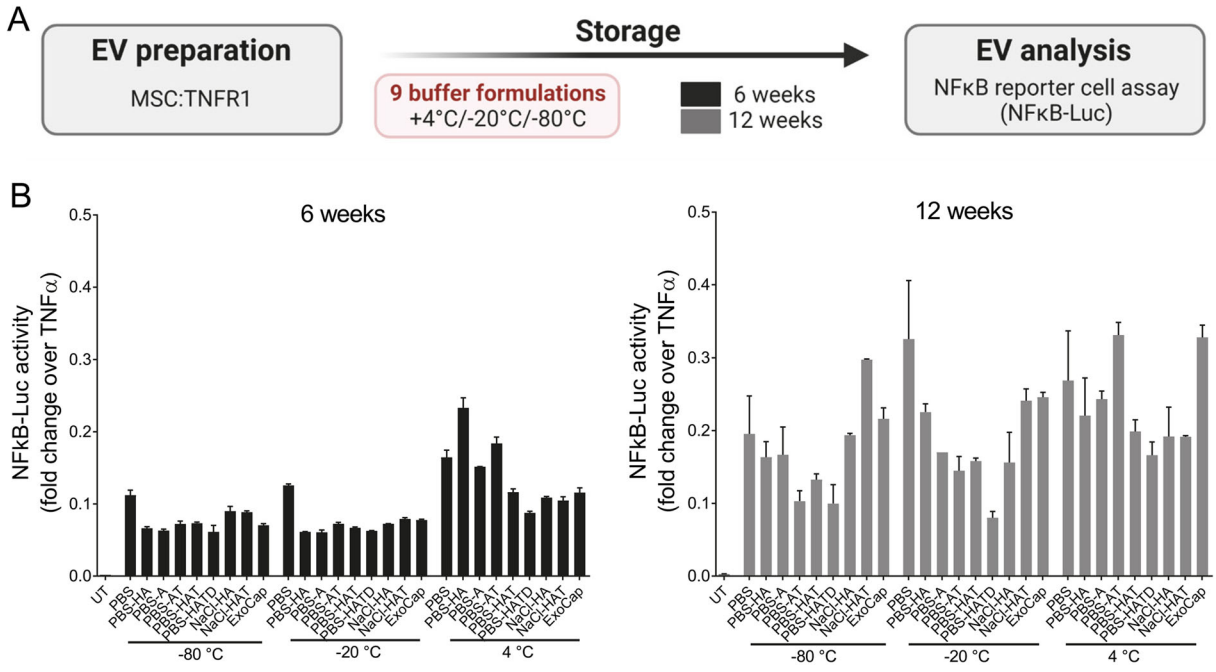

FIGURE 6 **Inhibitory functionality of engineered EVs displaying TNF-α binding decoy receptors**. (A) MSC:TNFR1 engineered decoy EVs were stored in respective buffers for 6, 12, and 20 weeks at +4˚C, -20˚C or -80˚C. (B) Equal volumes from aliquots were evaluated for TNF-α decoy in a reporter cell assay responsive to TNF-α induced NF-κB activation. Data were normalized to cells treated with TNF-α only (no EVs; 5 ng/ml; $n = 2$; mean±SD)

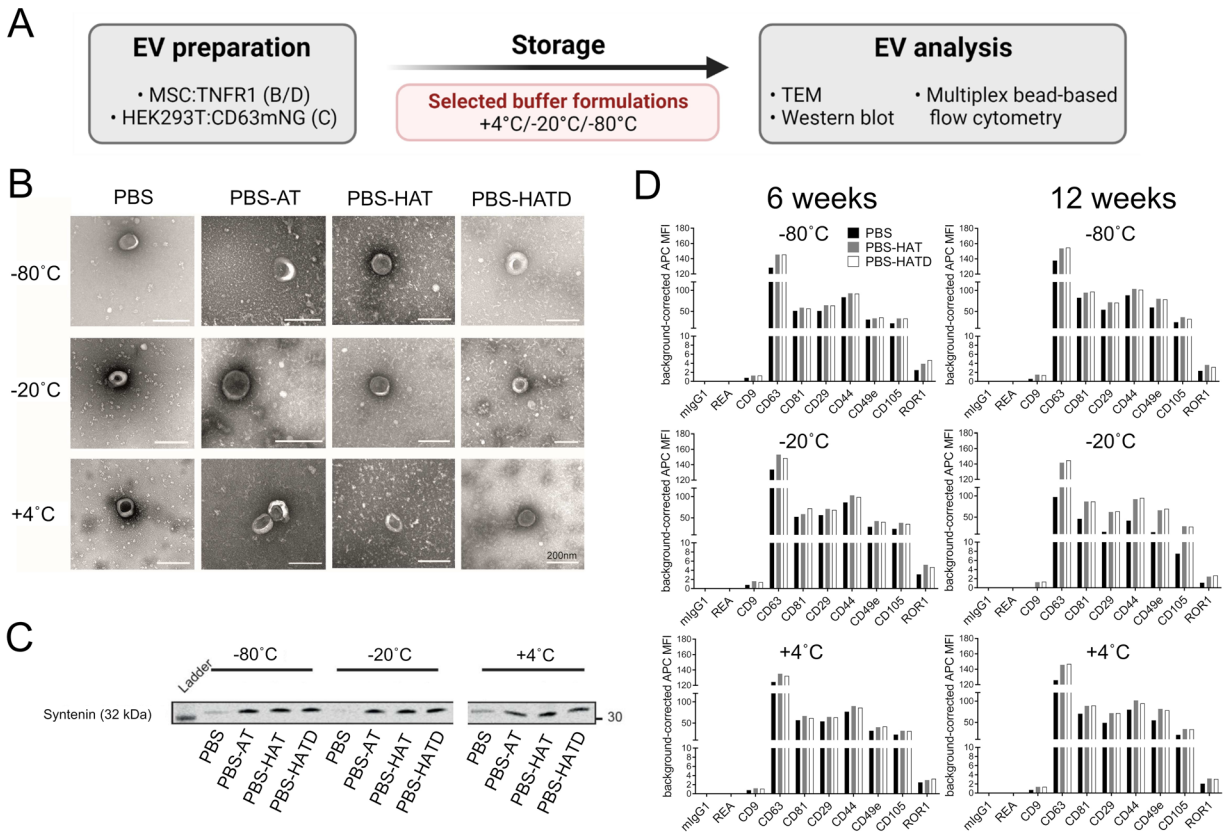

FIGURE 7 **Analysis of EVs stored in selected buffers by EM, WB and multiplex bead-based flow cytometry**. (A) MSC:TNFR1 engineered decoy EVs or HEK293T:CD63mNG derived EVs were stored in respective buffers 6–20 weeks at +4˚C, -20˚C or -80˚C before analysis. (B) Representative EM images of MSC:TNFR1 EVs after storage for 20 weeks. (C) Western blot analysis (anti-Syntenin) of equal volumes of HEK293T:CD63mNG EVs post storage for 20 weeks. Entire blot provided in Figure S3. Other EV-related proteins were tested but below detection limit for all samples. (D) Multiplex bead-based flow cytometry analysis of EVs stored for 6–12 weeks. A mixture of APC-labelled anti-CD9, CD63 and CD81 antibodies was used for detection. Background subtracted APC MFIs are shown. Equal volumes of 60 μl EV suspension from each aliquot were taken as assay input

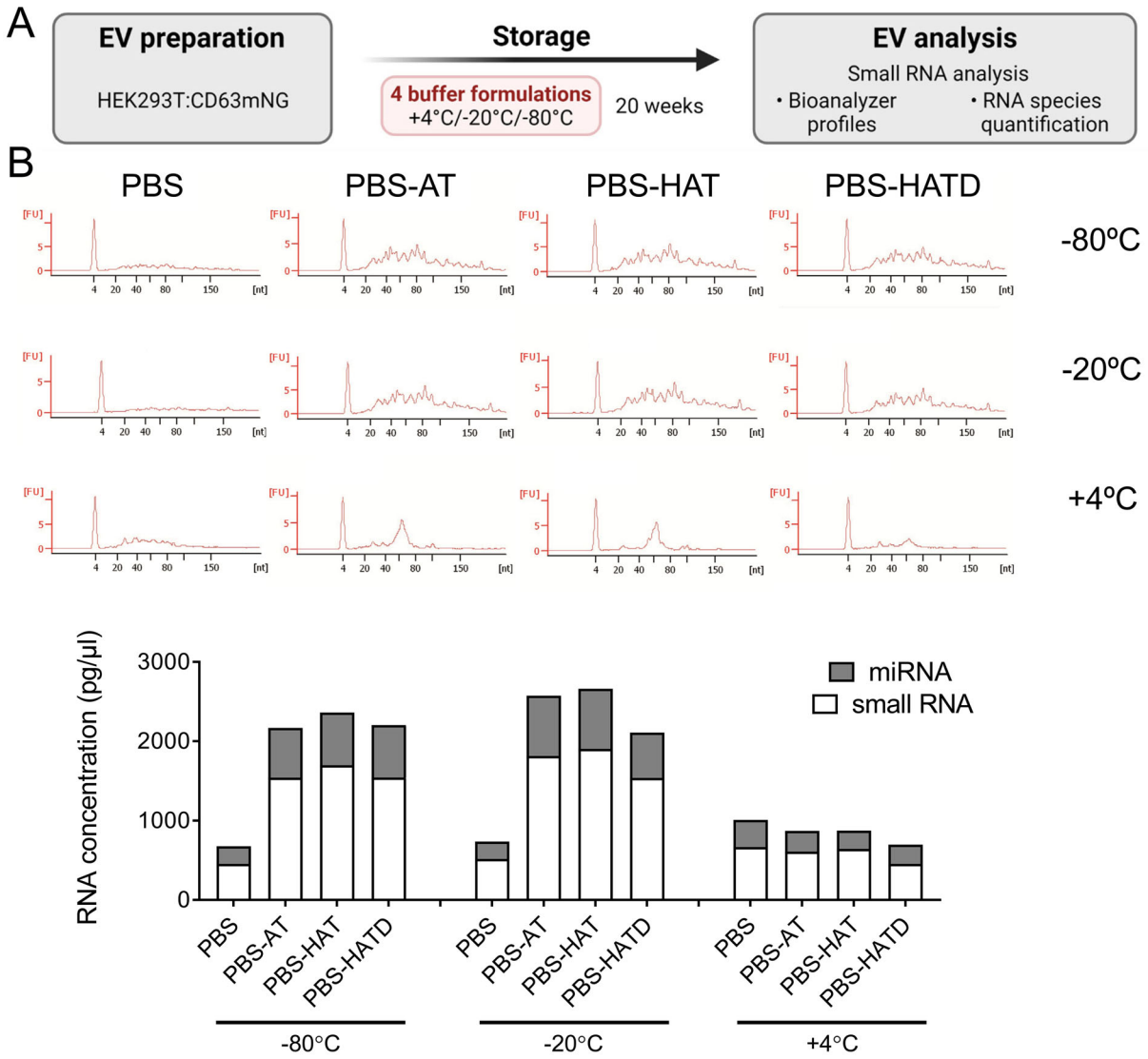

FIGURE 8 **RNA stability is severely affected when EVs are stored in PBS**. (A) RNA was analysed from HEK293T:CD63mNG derived EVs stored for 20 weeks. No data for fresh samples available. (B) Representative Agilent Bioanalyzer small RNA profiles and quantification of small RNA (5-200 bp, white) and miRNA (10-40, grey) concentrations of selected EV samples stored under different conditions

Data was analysed with FlowJo software (version 10.0.7). Mean fluorescence intensity was normalized over the control/untreated cell sample (ΔMFI).

2.9 | HEK NF-kb Luc reporter cell assay

NF-κB reporter (Luc)-HEK293 cells (BPS Bioscience, cat 60650) were seeded at a density of 3×10^4 cells per well in a 96-well plate and culture in DMEM supplemented with 10% FBS and 1% Anti-Anti. After 24 h, 50 µl of complete DMEM were mixed with or without MSC:TNFR1 EVs in combination with hTNF-α (5 ng/ml, NordicBiosite) and added to the cells. 6 h post-treatment the cells were lysed using 0.1% Triton X-100 diluted in PBS (Sigma) and mixed with D-Luciferin substrate (Promega) prior to luminescence measurement with GloMax-96 Microplate Luminometer (Promega) as described previously (Gupta et al., 2021).

2.10 | Western blot

Equal volumes of EV-containing samples were mixed with buffer containing 0.5 M dithiothreitol (DTT), 0.4 M sodium carbonate (Na2CO3), 8% SDS, 10% glycerol, blue bromophenol as loading dye and heated at 65°C for 5 min. Denatured and reduced samples were loaded on a NuPAGE® Novex® 4–12% Bis-Tris Protein Gel (Invitrogen, Thermo Fisher Scientific) and run at 120 V in NuPAGE® MES SDS running buffer (Invitrogen, Thermo Fisher Scientific) for 2 h. The proteins were transferred from

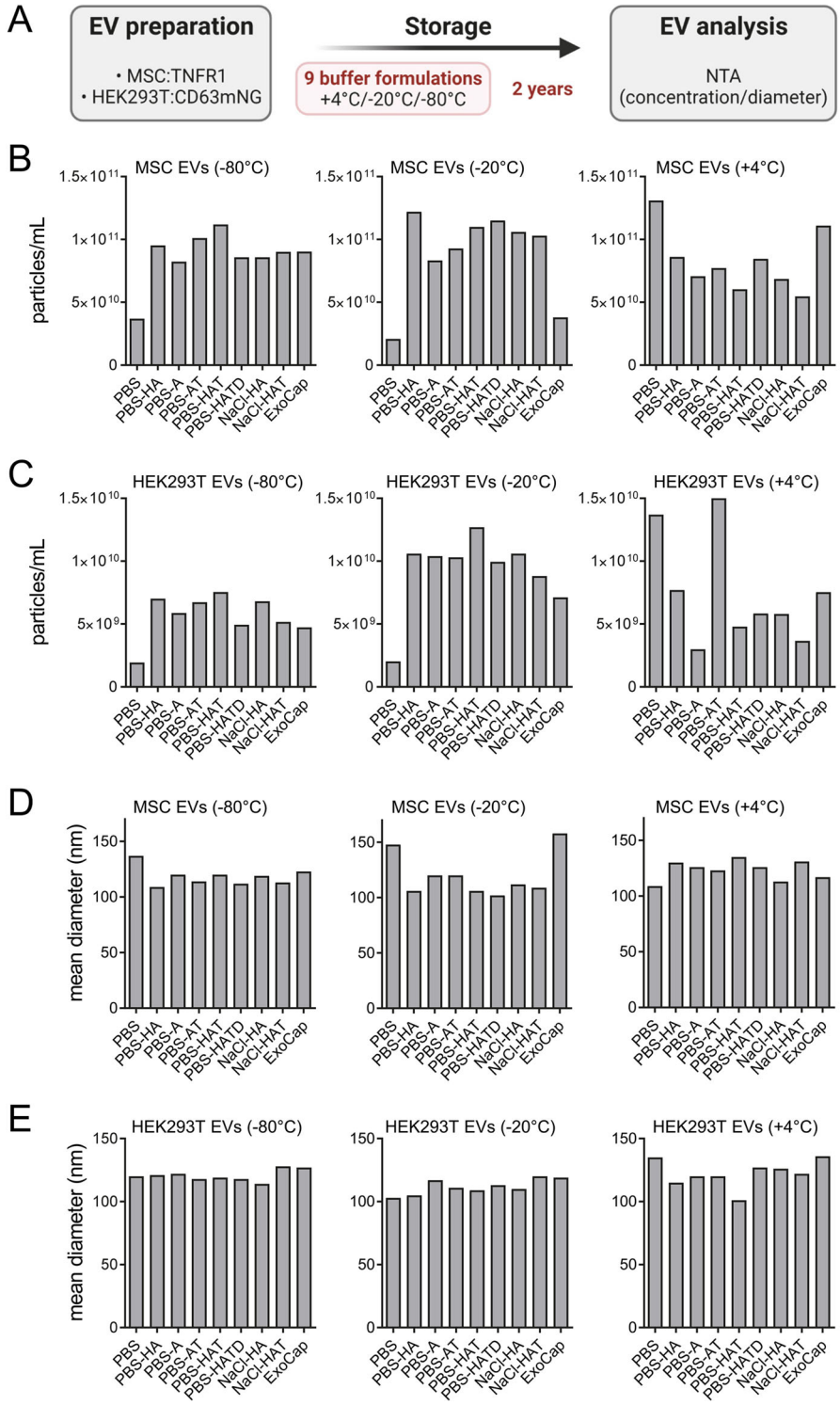

FIGURE 9 **NTA analysis of EV samples stored in different candidate buffers after 2 years.** (A) Measured particle concentration in MSC-TNFR EV aliquots. (B) Measured particle concentration in HEK293T:CD63mNG EV aliquots. (C) Particle diameters measured for MSC:TNFR1 EV aliquots. (D) Particle diameters measured for HEK293T:CD63mNG EV aliquots. All data is presented without normalization to freshly measured samples due to expected instrument performance variation after 2 years. Size distribution graphs are available in Figures S7 and S8

the NuPAGE gel to an iBlot nitrocellulose membrane (Invitrogen, Thermo Fisher Scientific) for 7 min using the iBlot system. The nitrocellulose membrane was blocked with Odyssey blocking buffer (LI-COR) for 60 min at RT with gentle shaking. After blocking, the membrane was incubated overnight at 4˚C with primary antibody solution (1:1000 dilution for anti-Syntenin (clone TA504796, Origene). The membrane was washed with PBS supplemented with 0.1% Tween-20 (PBS-T, Sigma) five times every 5 min and incubated with the secondary antibody (LI-COR) for 1h at RT (1:15,000 dilution of goat anti-mouse IRDye800CW).

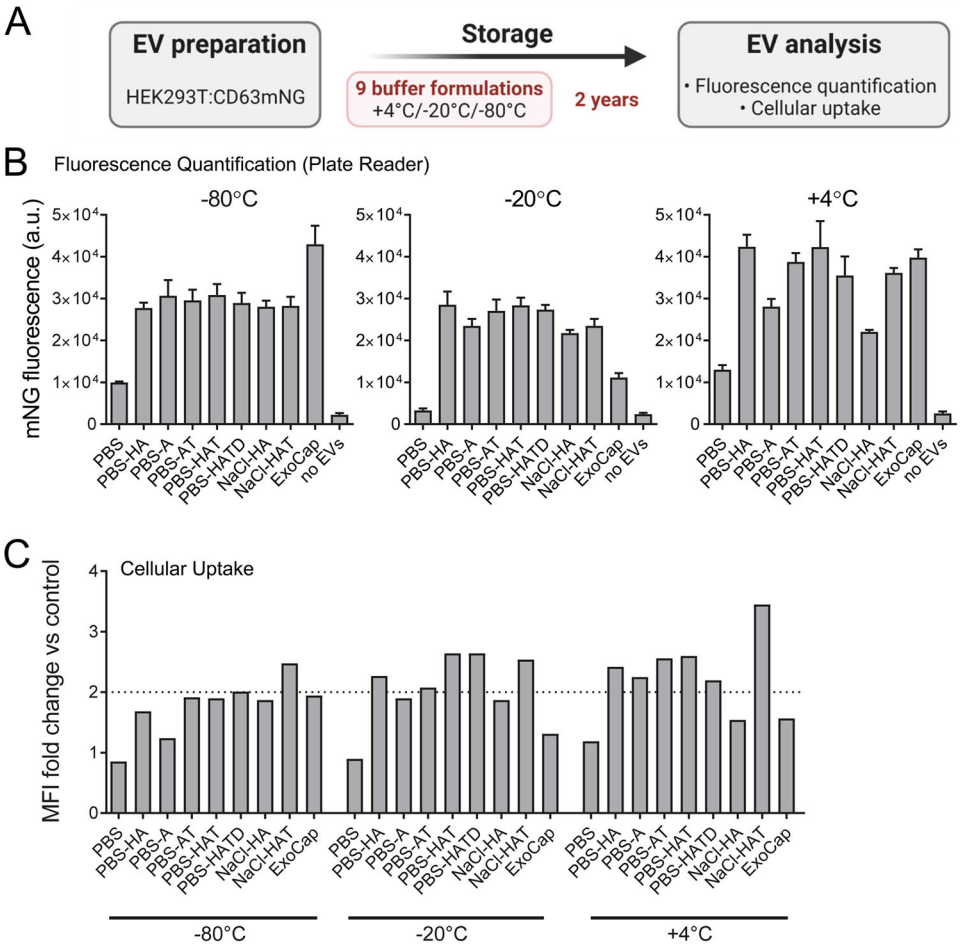

FIGURE 10 **Using fluorescence-tagged EVs to evaluate stability in various buffers after 2 years**. (A) HEK293T:CD63mNG engineered fluorescent EVs were stored in respective buffers for 2 years at +4˚C, -20˚C or -80˚C. Equal volumes from aliquots were subjected to bulk fluorescence measurements (B; $n = 2$; mean±SD) or cellular uptake assays (C)

The membrane was washed with PBS-T five times within 25 min, twice with PBS and visualized on the Odyssey infrared imaging system (LI-COR).

2.11 | Transmission electron microscopy

EV-containing aliquots were diluted in PBS and added onto glow-discharged formvar-carbon type B coated electron microscopy grids (Ted Pella Inc) for 30 s. The grids were blotted dry, washed with distilled water and dried again with filter paper. After the wash, the grids were stained with 2% uranyl acetate in double distilled H_2O (Sigma) for 10 s and filter paper-dried. The grid was air-dried and visualized on a transmission electron microscope (FEI Tecnai Spirit BioTwin) at 120 kV.

2.12 | In vivo biodistribution

EVs were isolated from HEK293T cell cultures by TFF/BE-SEC as described above and stored for 2 months in PBS-HAT buffer at -80˚C. After thawing, 2×10^{12} EVs were labelled with DiR (1,1-dioctadecyl-3,3,3,3-tetramethylindotricarbocyanine iodide, cat D12731, Life Technologies) O/N at 4°C in a total volume of 2 ml as described previously (Wiklander et al., 2015). In brief, EVs were injected intra-venously (tail vein) at doses of 2×10^{11} EVs in a volume of 100 μl per mouse ($n = 3$ C57BL/6 mice). Organs were analysed with IVIS 6 h post injection *ex vivo*. The animal experiments were approved by the Swedish Local Board for Laboratory Animals. The experiments were performed in accordance with the ethical permissions granted and designed to minimize the suffering and pain of the animals.

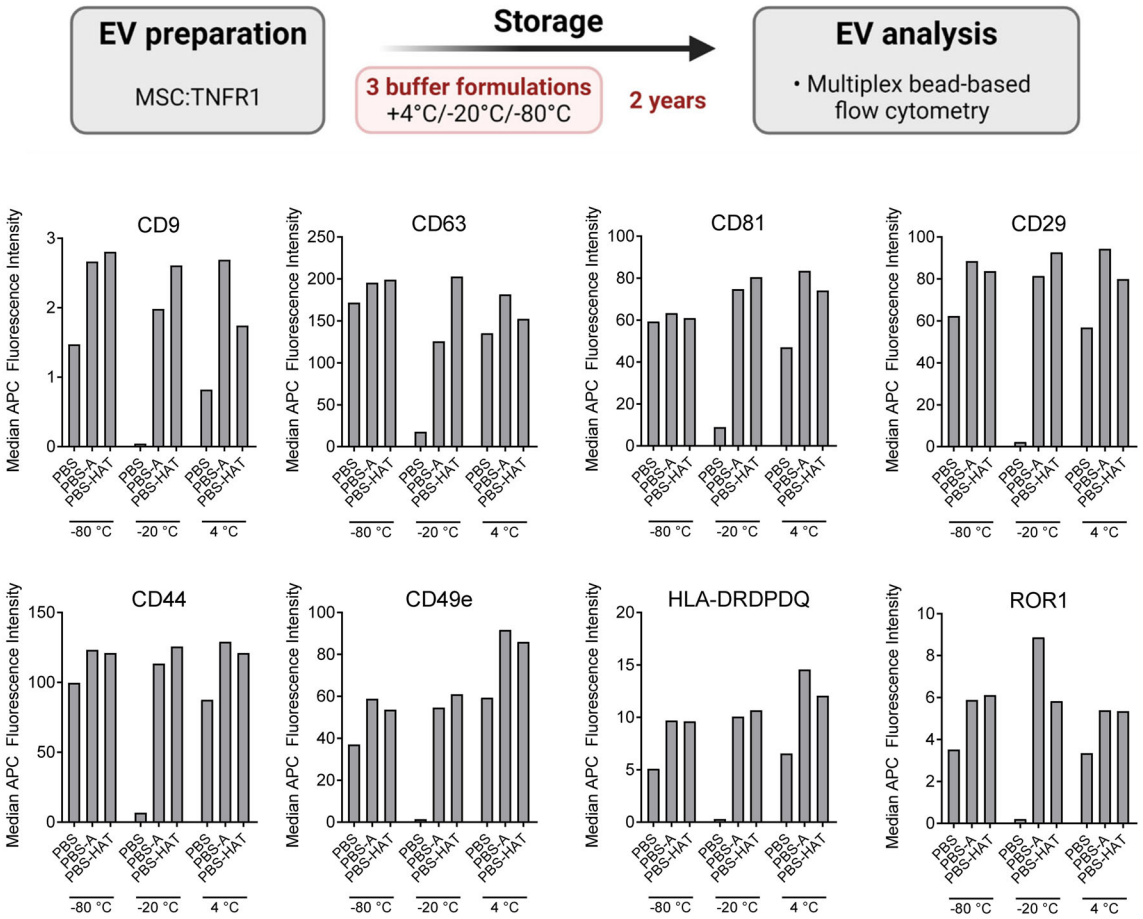

FIGURE 11 **Analysis of EVs stored for 2 years in selected buffers by multiplex bead-based flow cytometry**. Multiplex bead-based flow cytometry analysis of EVs stored for 6–12 weeks. A mixture of APC-labelled anti-CD9, CD63 and CD81 antibodies was used for detection. Background subtracted APC MFIs are shown for selected positive surface markers. Equal volumes of 60 μl EV suspension from each aliquot were taken as assay input. Full profiles are available as Figure S9

2.13 | Imaging flow cytometry analysis

EVs were analysed at the single vesicle level by high resolution Imaging Flow Cytometry (IFCM) on an Amnis Cellstream instrument (Luminex) equipped with 405, 488, 561 and 642 nm lasers) based on previously optimized settings and protocols established on an Amnis Imagestream X MkII instrument (Gorgens et al., 2019). For analysis of stored HEK293T:CD63mNG fluorescent EV samples (Stage 3; Figure 13B/S10A), a volume of 25 μl from each aliquot was diluted 500 fold in PBS-HAT buffer before analysis. Otherwise unlabelled MSC:TNFR1 EV aliquots were incubated with a mixture of APC-labelled anti-CD9 (Miltenyi Biotech, clone SN4), anti-CD63 (Miltenyi Biotec, clone H5C6) and anti-CD81 antibodies (Beckman Coulter, clone JS64) at a concentration of 8 nM over-night and diluted 1000 fold in PBS-HAT buffer before data acquisition. All antibodies were centrifuged for 10 min at 17,000 × *g* before usage. Samples were measured from 96 well U bottom multiwell plates (ThermoFisher Scientific) by using the plate reader of the Cellstream instrument with FSC turned off, SSC laser set to 40%, and all other lasers set to 100%. EVs were defined as SSC (low) by using neonGFP-tagged EVs as biological reference material, and regions to quantify mNG+ or APC+ fluorescent events were set according to unstained non-fluorescent samples and single fluorescence positive mNG-tagged reference EV controls as described before (Gorgens et al., 2019) (Figure S11). Samples were acquired for 5 min at a flow rate of 3.66 μl/min (setting: slow) with CellStream software version 1.2.3 and analysed with FlowJo Software version 10.5.3 (FlowJo, LLC). Dulbecco's PBS pH 7.4 (Gibco) was used as instrument sheath fluid. Absolute fluorescence calibration and presentation of fluorescence data in molecules of equivalent soluble fluorophores (MESF) was performed as described before (Gorgens et al., 2019; Tertel et al., 2020). In brief, FITC MESF beads (Quantum FITC-5 MESF, Bangs Laboratories Inc., cat 555A, lot 13734) and PE MESF beads (BD Quantibrite PE Beads, cat 340495, lot 49549) with known absolute fluorescence values for each bead population were acquired with the same settings used for EV measurements with the exception that the SSC laser was turned off, and linear regressions were performed to convert fluorescence values into FITC/APC MESF values, respectively. Flow cytometric

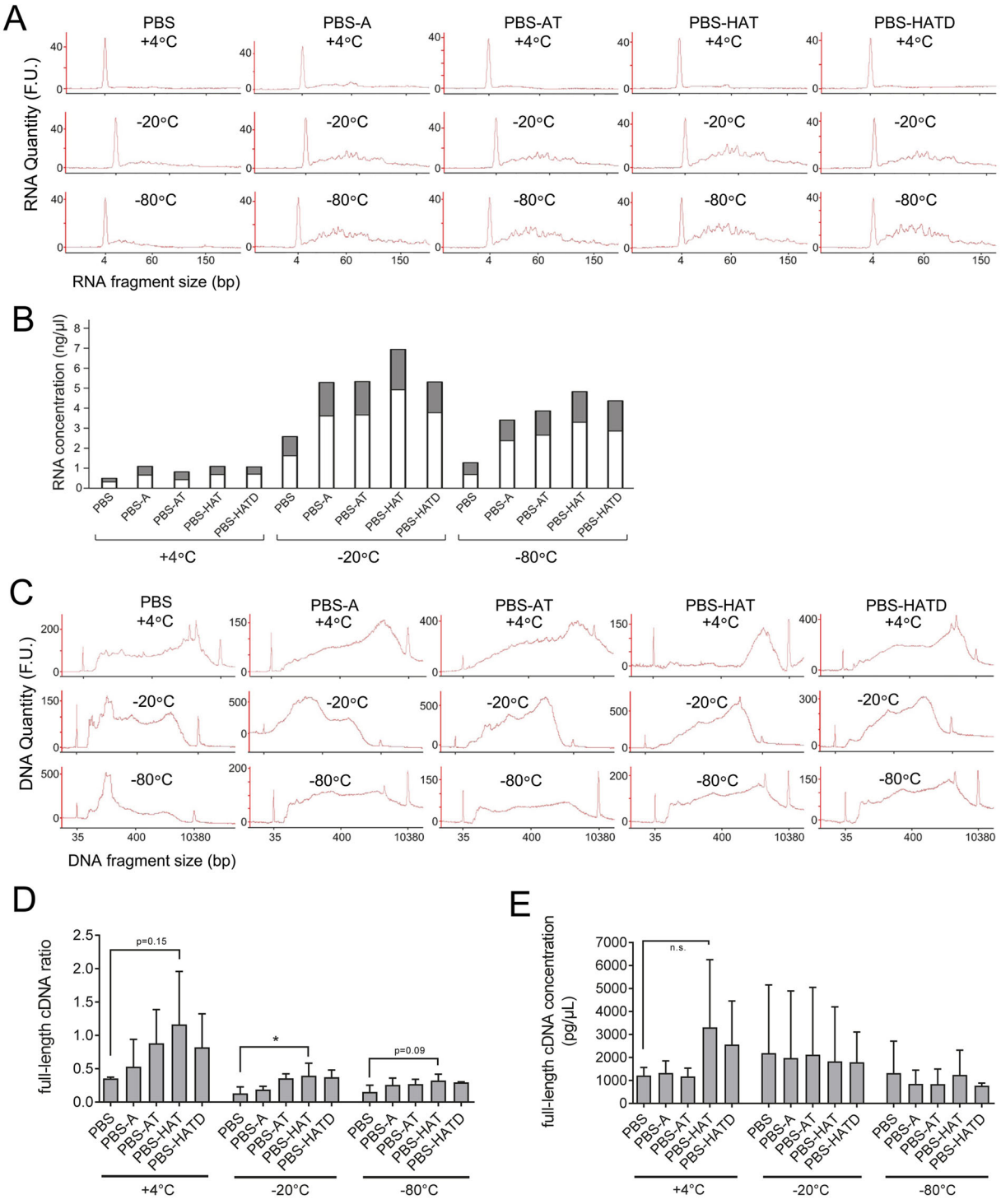

FIGURE 12 **Analysis of HEK293T:CD63mNG EV RNA after 2 years of storage under various conditions**. (A) Representative Agilent Bioanalyzer small RNA profiles following storage under different conditions. (B) Quantification of small RNA (white) and miRNA (grey) concentrations after storage under different storage conditions. (C) Representative Agilent Bioanalyzer HS DNA profiles of cDNA produced from RNA stored under different conditions. (D) The ratio of cDNA concentration 50–600 bp to that 0.6 to 10 kb from the cDNA profiles such as those presented in C was used to calculate mRNA stability under the different storage conditions ($n = 3$, mean±SD; *:$P < 0.05$). (E) Quantification of full-length cDNA from C (n.s.: $P > 0.05$). No values for fresh samples available. Statistical significance was assessed by one-way ANOVA followed by Dunnet's posthoc tests

TABLE 1 Stage 2 Buffer formulations

Buffer no.	Base buffer	HEPES	Albumin	Trehalose	DMSO	Glycerol	pH
1	PBS						7.00
2	PBS		+				6.80
3	PBS		+	+			7.00
4	PBS	+	+	+			7.00
5	PBS	+	+	+	+		7.00
6	PBS	+	+	+		+	7.00
7	PBS			+			7.00
8	0.9% NaCl		+				6.00
9	0.9% NaCl		+	+			6.00
10	0.9% NaCl	+	+	+			6.80
11	0.9% NaCl	+	+	+	+		6.80
12	0.9% NaCl	+	+	+		+	6.80
13	HBSS		+				6.00
14	HBSS		+	+			6.00
15	HBSS	+	+	+			7.10
16	HBSS	+	+	+	+		7.10
17	HBSS	+	+	+		+	7.00
18	RPMI1640		+				7.10
19	RPMI1640		+	+			7.10
20	RPMI1640			+			7.10
21	RPMI1640		+	+	+		7.10
22	RPMI1640		+	+		+	6.80
23	10% Glucose	+					3.90
24	10% Glucose		+				3.90
25	10% Glucose	+	+				3.90
26	IMDM			+			7.10
27	IMDM		+	+			7.10

Final concentration of additives: HSA 0.2 %; Trehalose 25 mM; HEPES 25 mM; DMSO 1%; Glycerol 30%.

plots using MESF unit axes were created with FlowJo v 10.5.3 (FlowJo, LLC). The same settings were applied to analyse liposome samples. Further details according to MIFlowCyt-EV guidelines (Welsh et al., 2020) are provided in Supplemental Tables 1 and 2.

2.14 | Data analysis and statistics

Unless indicated otherwise data are expressed as mean ± SD and statistical significance was assessed by one-way ANOVA followed by Dunnet's or Tukey's posthoc tests. Further details are provided in respective figure legends. Graphs and diagrams were assembled using GraphPadPrism 7 (GraphPadPrism Software).

3 | RESULTS

3.1 | Isolated EVs appear unstable over time when stored in PBS (Stage 1)

In the initial experiments aiming to study EV stability at different storage temperatures over time (referred to as 'Stage 1'), EVs were isolated by differential ultracentrifugation (UC) and stored in PBS at different temperatures (+4˚C, -20˚C or -80˚C). The EVs were subsequently assessed in terms of particle concentrations as well as bulk protein and RNA content (Figure 1A). When performing daily quantification of particle concentration and diameter of samples stored at +4˚C in PBS for up to 8 days,

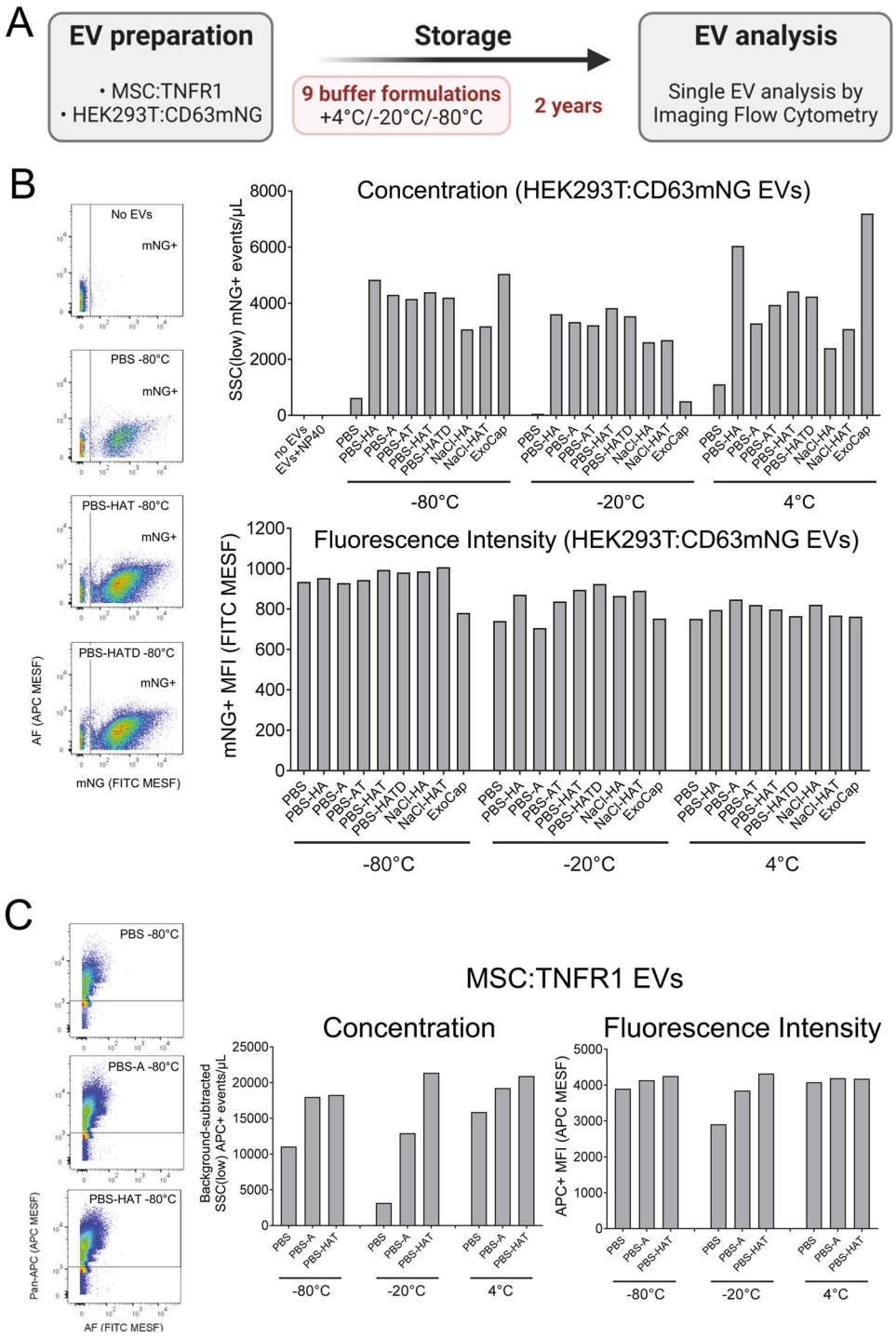

FIGURE 13 **EV quantification by high resolution imaging flow cytometry (IFCM) after 2 years of storage**. (A) EV samples after 2 years of storage in respective candidate buffers were subjected to IFCM analysis. Equal volumes from each aliquot were used accordingly. (B) IFCM analysis of fluorescently tagged HEK293T:CD63mNG EVs. Samples were diluted 500 fold in PBS-HAT before measurement. (C) 25 μl of MSC:TNFR1 EVs were incubated over-night with 8 nM of APC-labelled anti-CD9, anti-CD63 and anti-CD81 antibodies, respectively. Samples were diluted 1000 fold in PBS-HAT before data acquisition. Controls, gating strategy and dotplots for all samples are available as Figure S10. Further details provided in Figure Tables S1 and S2. AF: autofluorescence

decreasing particle concentrations and RNA amounts were observed within the first 2–3 days. However, particle size and bulk protein amounts appeared unaffected (Figure 1B). NTA analysis of samples stored in PBS at +4˚C, -20˚C or -80˚C for 1 week revealed gradually decreasing particle concentrations regardless of storage temperature. While protein amounts were still close to fresh values, detected RNA quantities decreased to around 50% of the initial values with the lowest recovery at +4˚C (Figure 1C). Next, the same measurements were performed after storing EVs at -20˚C in PBS for up to 26 weeks. Again, particle

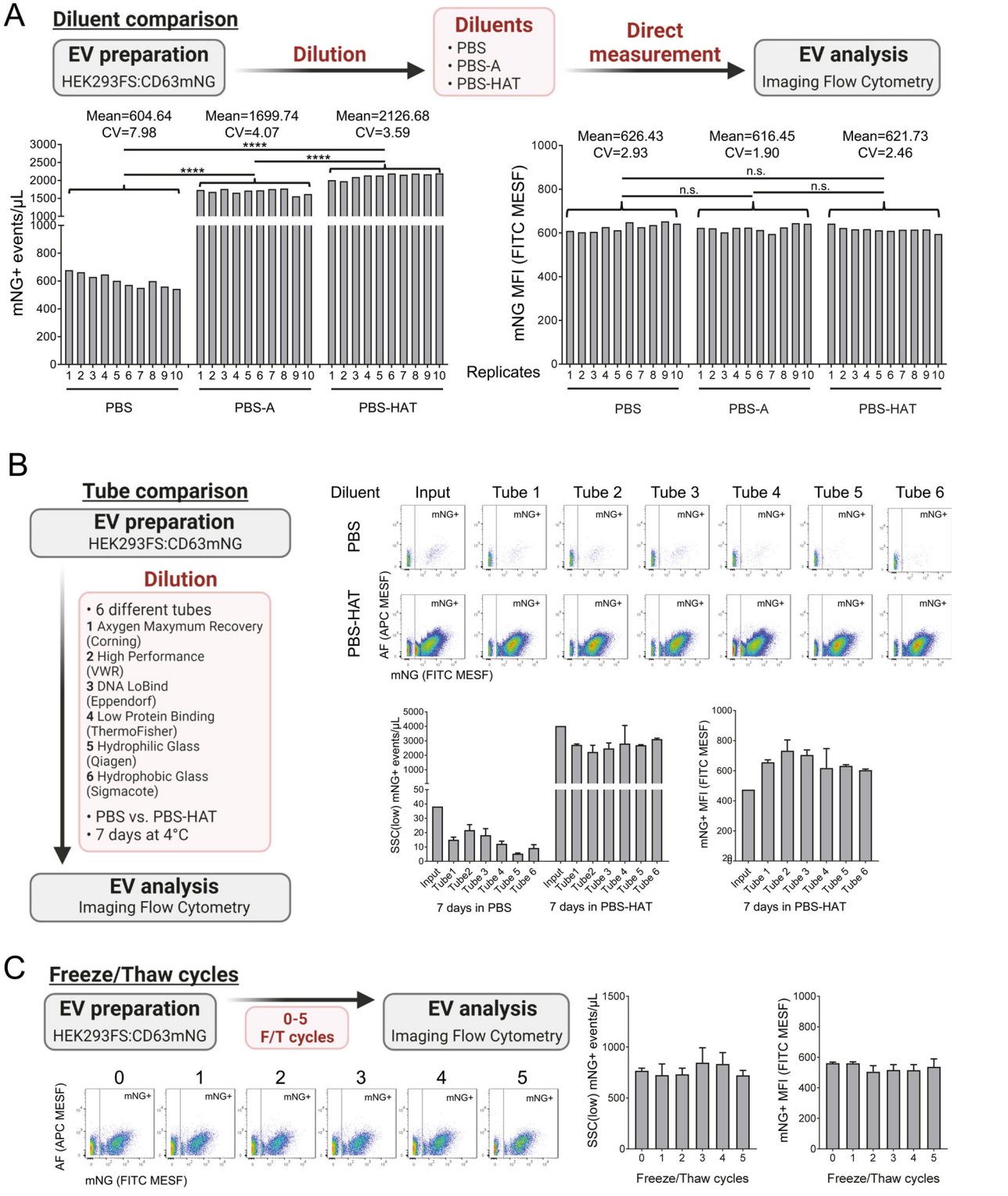

FIGURE 14 **Evaluation of the impact of diluent, tube type and freeze/thaw cycles on EV recovery.** (A) Fluorescently tagged HEK293-Freestyle EVs (HEK293FS:CD63mNG) were diluted 200,000-fold in either PBS, PBS-A, or PBS-HAT buffer and 10 replicates were acquired by IFCM for 180 s directly afterwards, respectively. Measured concentrations and fluorescence intensities are given in bar graphs, with replicate one measured first and replicate 10 measured last, respectively. (B) IFCM-based quantification of recovery of HEK293FS:CD63mNG EVs following storage of samples diluted 100,000 fold in PBS or PBS-HAT and stored for 7 days at +4°C in different tubes ($n = 3$). (C) HEK293FS:CD63mNG EVs measured freshly and after 1–5 freeze/thaw cycles by IFCM ($n = 3$). All data is expressed as mean±SD (n.s.: $P > 0.05$; ***: $P < 0.0001$; statistical significance was assessed by one-way ANOVA followed by Tukey's posthoc tests.). AF: autofluorescence. Further details and supplemental data provided in Figures S11-S13, and Tables S1 and S2

concentrations were decreasing from an approximate 70% reduction after 2 weeks to more than 90% loss at 26 weeks. A similar trend was observed with the protein content, with almost no proteins detected in samples stored longer than 8 weeks (< 5% of initial/fresh values). On the other hand, the mean particle diameters were gradually increasing from 109.7 (±1.5) nm to 134.7 (±7.7) nm (Figure 1D). Analogous data from EVs stored at -80˚C in PBS for up to 26 weeks showed a similar trend with less severe decline of particle concentration (~50% reduction at 26 weeks) and protein amount over time, and no substantial changes in mean particle diameters. RNA analysis revealed that only ~20% of the initial RNA measured in fresh samples was recovered after 26 weeks of storage at -80˚C in PBS (Figure 1E). To address the question if the UC isolation method itself caused this decreased recovery of EVs over time, we performed a similar set of experiments with EVs purified by UF/SEC stored in PBS at -20˚C or -80˚C for up to 12 weeks and observed overall similar tendencies (Figure 1F). In summary, these data show that storing EVs in PBS can lead to reduced sample stability and/or recovery at short-term and mid-term time points. This decreased recovery of EVs over time cannot be attributed to the isolation method and seems generally less drastic when EVs are stored at -80˚C compared to -20˚C stored samples. RNA recovery appeared to be severely affected especially at longer time points.

3.2 | Screening for storage conditions stabilizing EVs (Stage 2)

The results shown above clearly indicated that PBS is not suitable for storing EV samples, hence we decided to next test a series of different alternative buffer formulations summarized in Table 1. The pH of all 27 selected buffer formulations was measured before usage (Table 1). Base buffers, additives, and their concentration were chosen based on reagents classically used to stabilize cells or particle suspensions with a preference for reagents that are already clinically used.

Since decreasing NTA-based concentration values over time were consistently observed, and since NTA measurements would be more suitable to detect loss of sample or disruption of EVs compared to bulk RNA or protein measurements(Stage 1, Figure 1), we decided that NTA based particle concentrations and diameter estimates would be a suitable surrogate readout to screen for conditions stabilizing EVs and used NTA as read-out for this 'Stage 2' screening. The aim of this stage was to identify buffer candidates being potentially more suitable for storing EVs than PBS, before evaluating those candidates at higher detail in the next stage. Two different types of EVs were included for this 'Stage 2': EVs from an immortalized human MSC line and HEK293T:CD63eGFP EVs engineered to carry an intravesicular fluorescent eGFP tag fused to the N-terminus of CD63. EVs from both cell sources were prepared by tangential flow filtration/ultrafiltration (TFF/UF) including a PBS-based diafiltration step, diluted 10-fold in the respective buffer indicated in Table 1, and then aliquoted and stored at +4˚C, -20˚C or 80˚C. This isolation approach was chosen as rather fast and scalable solution to produce the amount of EVs required for all planned aliquots. Samples were subjected to NTA analysis directly (fresh) and after storage for 5 and 15 weeks (Figure 2A). NTA analyses of nonEV containing buffers were performed as well for control purposes; however, the number of particles detected was neglectable for all buffers, that is, at similarly low levels as observed for plain PBS (data not shown). For NTA analysis of HEK293T:CD63eGFP EV aliquots, samples were additionally checked visually in fluorescence mode. To minimize delays during measurements and since eGFP fluorescence signals tend to fade quickly over time which results in more variable data (Corso et al., 2017), we decided to not record fluorescence signals but only scatter signals. For HEK293T:CD63eGFP EVs stored in buffers 6, 12, 17 and 22–25 (formulations based on Glucose and Glycerol), fluorescence NTA assessment revealed complete lack of eGFP fluorescence directly after diluting the sample in buffer (not shown). Since this might indicate EV instability or at least would compromise downstream analytical assays, all samples prepared in those buffers were excluded from further measurements. Overall, no consistent changes regarding EV diameter measured by NTA were detected for all samples (Figure S1).

For most buffers tested, the particle concentrations were decreasing over time in a temperature-dependent manner, and overall the particle loss appeared more pronounced for MSC EVs (Figure 2D-F) than for HEK293T EVs (Figure 2B/C). Particularly particle concentrations from MSC-EV samples were in average reduced most drastically at +4˚C and appeared least affected at 80˚C. PBS-stored EVs showed a similar decline (Figure 2), however, less pronounced than previously observed (Figure 1), and temperature independent. Measurements of HEK293T EVs showed increased concentrations after 15 weeks in three cases which were treated as outliers (Figure 2B, Buffers 3 and 21; Figure 2C, Buffers 9 and 11).

We further identified several buffers that appeared to improve EV stability and recovery over time. Based on particle concentrations measured, storing EVs at -20/80˚C in buffer formulations 3, 4, 5, 10, 13, 14, 16 and 21 seemed to stabilize EVs best. Storing EVs frozen in PBS supplemented with albumin (Buffer 2) showed consistent stabilizing effects compared to PBS alone (Buffer 1), which is in line with previous reports showing increased recovery rates in the presence of albumin (van de Wakker et al., 2021; Yamashita et al., 2016; Zhang et al., 2020). Moreover, adding further additives such as trehalose (Buffer 3), HEPES (Buffer 4) or DMSO (Buffer 5) appeared to further improve EV recovery rates when samples were frozen (Figure 2B/C/E/F). Considering these potentially beneficial effects on EV recovery after storage and since buffers devoid of albumin (Buffers 7, 20, 26)

appeared to be generally less stabilizing, we selected buffers 2, 3, 4, 5 and 10 as EV storage buffer candidates for further in-depth evaluation.

3.3 | In-depth evaluation of candidate EV storage buffer formulations (Stage 3)

In Stage 3, we decided to characterize the impact of several candidate buffers and PBS comprehensively with a variety of others state-of-the-art EV characterization methods and over a longer timeframe (Figure 3A). Of note, samples included in Stage 2 contained EVs enriched from cell culture supernatants by TFF/UF; however, samples prepared this way are less pure and contain a higher degree of residual free proteins compared to UC/SEC purified EVs analysed in Stage 1 (Figure 1). Taking this different degree of purity into consideration together with the observations of less drastically reduced particle concentrations stored in PBS in stage 2 compared to stage 1, and considering that albumin addition appears to stabilize EVs, our data so far implies that sample purity and protein content has a direct effect on EV stability and recovery after storage in PBS. For Stage 3, we thus decided to enrich EVs again by TFF/UF and purify samples additionally by Bind-Elute Size Exclusion Chromatography (SEC) as described previously (Corso et al., 2017).

In order to facilitate evaluation of parameters related to general integrity and functionality of stored EVs in addition to basic parameters such as particle concentration and size measured by NTA, we decided to perform stability experiments with two different types of engineered EVs: MSC-TNFR EVs engineered to suppress TNF-α signalling (Gupta et al., 2021) and HEK293T:CD63mNeonGreen EVs engineered to carry an intravesicular green fluorescent mNeonGreen (mNG) tag. EVs from both cell sources were prepared by TFF/UF including a PBS-based diafiltration step and purified by BE-SEC. This procedure resulted in relatively pure EVs in terms of particle-to-protein ratio for Stage 3 (1.14×10^9 particles/μg protein) compared to the EVs prepared for Stage 2 by TFF/UF only (2.85×10^6 particles/μg protein). EVs were diluted 10-fold in the respective buffer indicated in Figure 3A and then aliquoted and stored at +4˚C, -20˚C or -80˚C. Samples were analysed directly (fresh) or after 6, 12 and 20 weeks by NTA and several other state-of-the-art methods (Figure 3B).

3.4 | Evaluation of candidate EV storage buffer formulations after 6, 12 and 20 weeks

We subjected aliquots at given time points to NTA and compared measured concentrations to fresh values for all conditions (Figure 4A). Similar to Stage 1 and 2 results, storing EVs in PBS resulted in a clearly reduced recovery and a clear downwards tendency over time, with an overall loss of 30–80% of particles after 20 weeks (Figure 4B). The observed recovery of HEK293T derived EVs based on measured particle concentrations appeared to be reduced more severely in general than MSC derived EVs. Compared to PBS, all other eight candidate buffers included in this stage showed higher particle recovery at least when storing EVs at -80˚C. Storage of EVs in PBS-AT, PBS-HAT and PBS-HATD for 20 weeks resulted in the highest particle recovery for both MSC EVs (~80%) and HEK293T EVs (~50-60%). Using NaCl-HAT as storage formulation appeared to preserve particles well for MSC EVs (~80%) but less good compared to the other buffers for HEK293T EVs (~40%) (Figure 4B). No consistent changes of particle diameters estimated by NTA were observed (Figure S2).

3.5 | Evaluation of the stability of fluorescently tagged engineered EVs over time

Using fluorescently tagged EVs for analysis allows for detection of fluorescent events, thereby increasing confidence that actual EVs and not merely particles are analysed. We have previously shown that fluorescently tagged EVs are useful as reference material or for control purposes in various methods (Corso et al., 2017; Corso et al., 2019; Gorgens et al., 2019; Wiklander et al., 2018). Since the engineering locates the mNG fluorophore at the intravesicular part of CD63, fluorescence stability can further provide information about the intactness of engineered EVs. Thus, we next used fluorescently tagged HEK293T-mNG EVs to evaluate stability based on their fluorescence over time, both by direct fluorescence quantification in a plate reader and in a cellular uptake assay we have used in previous studies (Corso et al., 2017) (Figure 5A). Measured bulk fluorescence of EVs stored in PBS was consistently lower compared to all other included buffers, with only ~20-40% of initial fluorescence intensities measured. Particularly for EVs stored in buffers PBS-A, PBS-AT, PBS-HAT and PBS-HATD we detected levels of fluorescence comparable to values from fresh EVs for samples stored at all three temperatures, with no consistent downtrend. For EVs stored in ExoCap buffer rather higher fluorescence values than measured for fresh EVs were measured (Figure 5B). Similarly, we observed consistently lower and down trending values over time in cellular uptake assays for EVs stored in PBS, while EVs stored in most of the other eight included buffers yielded overall more stable and, in some cases particularly for the 20 weeks time point, even higher values compared to fresh measurements at all temperatures, the reason being unclear. (Figure 5C).

3.6 | Assessment of the stability of EV surface functionality using decoy receptor engineered EVs

An ideal storage buffer formulation wouldn't only facilitate stable recovery of numbers of EVs and their size and cargo, but also preservation of their surface composition. In another study, we recently described engineered therapeutic EVs displaying cytokine binding domains which can act as decoys for pro-inflammatory cytokines (Gupta et al., 2020). The MSC-TNFR1 EVs included in this Stage were consequently used to assess the ability of those EVs to decoy TNF-α over time, after storing EVs in different buffer formulations. As described previously (Gupta et al., 2021), we used an in vitro reporter system for TNF-α signalling based on detection of luciferase activity driven by a NF-κB minimal promoter and pre-mixed EVs with TNFα before adding them to reporter cells (Figure 6A). At all time points, we observed inhibitory activity for TNF-α decoy EVs compared to non-EV containing controls. EVs stored in PBS and to some extent EVs stored in ExoCap buffer consistently showed less inhibitory activity. In summary, buffers PBS-A, PBS-AT, PBS-HAT, and PBS-HATD were ranking best in terms of inhibitory activity throughout this experimental series (Figure 6B).

3.7 | Characterization of EVs stored in selected candidate buffers by electron microscopy, Western blot, and bead-based multiplex flow cytometry

EVs are relatively complex entities and contain a multitude of different molecules both on the outside and inside. Combined with our still limited understanding of different EV-mediated functions and their heterogeneity, this makes it overall difficult to accurately assess EV intactness and stability. Thus, we decided to further characterise EVs stored in selected candidate buffers at -80˚C, -20˚C and +4˚C by other orthogonal EV characterization methods at selected time points as far as material was available (Figure 7A). TEM analysis of MSC-TNFR EVs stored for 20 weeks did not reveal any consistent storage buffer-related difference in EV shape, diameter, or intactness; however, relatively low EV concentrations precluded quantitative analysis (Figure 7B). Western blot analysis of the EV-related protein Syntenin showed clearly reduced expression in HEK293T:CD63mNG EVs stored in PBS compared to PBS-AT, PBS-HAT and PBS-HATD for all three temperatures (Figure 7C). Multiplex bead-based flow cytometry, an EV specific immune-capture assay recently optimized by us and others (Koliha et al., 2016; Wiklander et al., 2018), showed robust bulk detection of all typical HEK293T EV surface proteins for EVs stored in PBS, PBS-HAT and PBS-HATD, however, signals were consistently lowest for EVs stored in PBS (Figure 7D).

3.8 | Evaluation of stability of EV associated small RNA after storage for 20 weeks

Many studies indicate that in addition to biophysical parameters and proteins, RNA contents of EVs can play an important role in their function (Mateescu et al., 2017), and thus any storage condition stabilizing EVs should ideally also preserve their RNA cargo. Here, we quantified smallRNA from HEK293T:CD63mNG EVs stored in selected buffers (PBS, PBS-AT, PBS-HAT and PBS-HATD) at -80˚C, -20˚C and +4˚C and analysed their small RNA profiles (Figure 8A). We consistently measured lower smallRNA amounts for EVs stored in PBS at all temperatures while profiles for EVs stored in PBS-AT, PBS-HAT, PBS-HATD appeared to be less affected at -80˚C and -20˚C (Figure 8B). The amount of detectable smallRNA for samples stored at +4˚C was overall lower for all samples. Due to the lack of data on fresh EVs the extent of smallRNA reduction cannot be quantified; however, this suggests that smallRNA integrity is dependent on similar parameters to that of EVs, such that samples stored at higher temperatures without stabilizing reagents are subject to degradation.

3.9 | In-depth evaluation of EV stability in PBS-HAT buffer at -80°C

Based on all results to this point, we here selected the buffer PBS-HAT as default buffer since EVs appeared to be most stable at all conditions up to 20 weeks. In order to minimize the potential for unwanted downstream effects on EV experiments, we further evaluated effects of the PBS-HAT buffer on EV stability and function. First, to investigate potential buffer-mediated effects on cellular assays, we compared the transcriptional response of fibroblast cultures treated with PBS-HAT buffer alone or HEK293T EVs stored in PBS-HAT buffer to untreated fibroblasts (Figure S4). Comparison of transcriptomes of individual samples with different methods revealed that PBS-HAT treated and untreated fibroblasts clustered closely together, while treatment of fibroblasts with HEK293T EVs resulted in a clearly changed and distinct transcriptome compared to both untreated and PBS-HAT treated fibroblasts. Moreover, differential expression analysis detected only two significantly downregulated genes following treatment with PBS-HAT, in comparison to thousands of differentially regulated genes when cells were exposed to EVs. This indicates that PBS-HAT buffer itself does not notably impact cellular transcriptomes in cell-based assays (Figure S4).

Next, we addressed if storing EVs in PBS-HAT buffer would impact mouse biodistribution experiments which are regularly performed in our lab with engineered EVs to evaluate their therapeutic potential. In a proof-of-concept biodistribution experiment we observed distribution patterns of EVs stored in PBS-HAT similar to previously reported experiments with fresh EVs (Wiklander et al., 2015) (Figure S5). We didn't include a direct comparison of stored versus fresh EVs here due to sample availability; however, these results provide evidence that storage of HEK293T EVs in PBS-HAT does not change their typically observed general biodistribution patterns in mouse experiments.

Finally, we evaluated the stability of EV preparations stored in PBS-HAT buffer by performing NTA analysis freshly and whenever samples were thawed and used for experiments. NTA data was collected for a total of 74 independent EV preparations stored in PBS-HAT at -80°C for 7 to 251 days. In a correlation analysis of NTA fold change particle concentrations (fresh/post-thaw) versus storage time (Figure S6A) or versus initial particle concentration (Figure S6B), we did not observe any correlation, respectively. This indicates that neither storage time within the assessed timeframe nor initial particle concentration in the analysed range are affecting EV stability when PBS-HAT is used as storage buffer.

3.10 | Evaluation of long-term storage (2 years) effects under various conditions

The data shown above demonstrates that most candidate buffers improved the recovery of EVs after storage times up to 20 weeks drastically compared to plain PBS. Even though we already had selected PBS-HAT (at -80°C) as default EV storage buffer, we decided to follow up sample stability and EV recovery at one long-term storage time point and analysed aliquots of the same EV batch after 2 years of storage. Due to more limited comparability to previous measurements in most assays (e.g., due to instrument modifications and realignment and new reagent batches resulting in overall data variation) and the lack of available or applied routines for absolute data calibration at the time, all data at 2 years are presented separately and values are not normalized to fresh values.

NTA-based particle concentrations at -80°C were generally lowest when using PBS and about 2–3 fold higher in all other candidate buffers, with highest concentrations detected in PBS-HAT buffer, both for MSC and HEK293T EVs (Figure 9B/C). Particle concentrations for EVs stored at -20°C were decreased even more drastically (5-6 fold) when stored in PBS compared to most other buffers tested, with the exception of ExoCap buffer which also showed a clear reduction for both MSC and HEK293T derived EVs (Figure 9B/C). Obtained particle diameters were overall comparable for all aliquots between temperatures for both MSC and HEK293T derived EVs; however, we observed overall increased variation of measured particle diameters particularly for MSC EVs stored in PBS and ExoCap buffer (Figure 9D/E).

Next, we utilized HEK293T:CD63mNG derived fluorescently tagged EVs as before and quantified bulk fluorescence in, respectively, stored EV samples directly, and performed cellular uptake assays based on fluorescence measured by flow cytometry (Figure 10A). Bulk fluorescence was drastically reduced for samples stored in PBS at all temperatures, most severely for samples stored at -20°C. Results after storage in ExoCap buffer and at +4°C appeared generally more variable; however, samples stored in most other candidate buffers (PBS-HA, PBS-A, PBS-AT, PBS-HAT, PBS-HATD) showed relatively constant bulk fluorescence signals both at -80°C and -20°C (Figure 10B). In cellular uptake experiments we observed undetectable (fold change ≤1; -80°C/-20°C) or extremely low (fold change: 1.19; +4°C) uptake values when using PBS-stored EVs, but values in a similar fold change range as observed for fresh EVs (fold change: 2.0) for several other buffers at all temperatures, in particular for PBS-AT, PBS-HAT, and PBS-HATD (Figure 10C).

Multiplex bead-based flow cytometry analysis of MSC-TNFR EV samples stored in selected buffers (PBS, PBS-A, PBS-AT) for 2 years revealed clearly reduced (80°C/+4°C) or drastically reduced (-20°C) detection of EV surface markers when EVs were stored in PBS. Obtained values for EVs stored in PBS-HAT were comparable to PBS-A stored samples (Figure 11).

Next, we evaluated RNA stability for EV samples stored for 2 years in respective candidate buffers. We prepared profiles of small RNA species as before, and this time additionally amplified full-length cDNA from mRNA contained in EV samples. Small RNAs were clearly most degraded following storage in PBS for all temperatures compared with other candidate buffers tested (PBS-A, PBS-AT, PBS-HAT, PBS-HATD), and we observed generally less degradation for frozen samples (-20/80°C) compared to EVs stored at +4°C (Figure 12A/B). When comparing samples stored at respective temperatures, EVs stored in PBS-HAT buffer in all cases showed the least pronounced signs of RNA degradation amongst the candidate buffers tested (Figure 12B). Analysis of full-length cDNA amplified from the same set of samples generally revealed highest full-length ratios for EV samples at +4°C; however, the absolute amount of RNA detected was higher for frozen samples, respectively. mRNA appeared to be least stable post storage in PBS for all temperatures, and full-length cDNA ratios appeared to be highest for PBS-HAT stored EVs at all temperatures (Figure 12C-E).

3.11 | Analysis of EVs following 2 years of storage by high resolution imaging flow cytometry

In order to further assess quality and quantity changes in, respectively, stored samples, we next applied high resolution EV analysis by imaging flow cytometry (IFCM), a method we and others have established and optimized in recent years (Gorgens et al., 2019; Lannigan & Erdbruegger, 2017; Tertel et al., 2020). IFCM facilitates EV protein analysis through the introduction of fluorescent tags or usage of fluorescently labelled antibodies together with robust EV quantification, at the single EV level. Here, we now analysed HEK293T:CD63mNG EVs and MSC-TNFR EVs after 2 years of storage by IFCM and quantified EV concentration and fluorescence intensity for EVs stored in the different candidate buffers at the different temperatures, respectively (Figure 13A). Confirming previous results, analysis of fluorescently tagged HEK293T:CD63mNG EVs revealed drastically reduced concentrations of fluorescent EVs following storage in PBS across temperatures. The mean brightness per EV was overall higher at 80°C compared to -20°C and +4°C and appeared most variable at +4°C. EV storage in buffers PBS-HAT and PBS-HATD overall yielded the most consistent concentration measurements throughout all three temperatures (Figure 13B, Figure S10). MSC-TNFR EVs stored in PBS, PBS-A or PBS-HAT were analysed after staining with a combination of fluorescently labelled antibodies against the tetraspanins CD9, CD63 and CD81. Again, the analysis showed a reduction in concentration of total tetraspanin-positive EVs after storage in PBS, most severely at -20°C. This reduction was milder when EVs were stored in albumin-supplemented PBS (PBS-A). Highest values were measured for EVs stored in PBS-HAT buffer which additionally contained trehalose/HEPES (Figure 13C).

In summary, the IFCM analysis of EVs stored for 2 years revealed even more drastically reduced recovery for PBS-stored EVs compared to the 20 weeks time point evaluated before, for both MSC and HEK293T derived EVs. Several other candidate buffers including PBS-HAT prevented this time-dependent decline when stored at -80°C.

3.12 | Evaluation of the impact of diluent, tube type and freeze/thaw cycles on EV recovery

Our results clearly indicate that the buffer formulation used to store EVs can drastically impact the quantity and quality of the recovered EVs. The changes observed could partly be explained by physical changes to EVs, for example, fusion, aggregation or disruption; however, the observation that the mean particle diameters did not notably change for samples with drastically reduced particle/EV numbers indicates that a significant portion of EVs might be bound to the plastic surfaces of tubes or pipet tips and thus are not recovered.

To further investigate this 'loss' of EVs through handling and plastic exposure, we next evaluated the impact of different candidate buffers during EV sample dilution. Starting with a relatively concentrated sample of HEK293FS:CD63mNG EVs (1×10^{12} particles/ml) in PBS-HAT, the sample was diluted 200,000-fold either in PBS, PBS-A, or PBS-HAT buffer and the mNG fluorescence positive (mNG+) EVs for each sample were immediately quantified by IFCM. Samples diluted in PBS showed about 2.8-fold less mNG+ EVs compared to PBS-A and 3.5-fold less mNG+ EVs compared to PBS-HAT. The measured concentration for EVs diluted in PBS was further declining over the measurement of the 10 replicates, indicating rapidly progressing plastic adhesion of EVs while measurements appeared stable for EVs diluted in PBS-A or PBS-HAT. The fluorescence intensity of mNG+ EVs did not change over time and was similar for samples diluted in the different buffers, indicating that EVs are not aggregating or disrupted, but rather stochastically binding to plastic over time when stored in PBS, but not in PBS-A or PBS-HAT (Figures 14A and S11). In a similar dilution experiment additionally including PBS supplemented with Trehalose alone (PBS-T) we observed the same decline in recovered EVs as in PBS, indicating that the addition of Trehalose alone is not sufficient to prevent the observed loss (Figure S12).

These drastic changes within minutes of EV handling when using PBS (or PBS-T) as diluent underline the importance of using more suitable buffers like PBS-HAT for dilution steps in any downstream EV assay, and not only for storage purposes. To investigate if this reduced recovery is specific for EVs, we performed a corresponding set of experiments with fluorescently labelled liposomes. Similar to EVs before, samples diluted in PBS or PBS-T showed ~1.9-fold less liposomes compared to PBS-A and ~2-fold less liposomes compared to PBS-HAT when quantified by IFMC directly after dilution (Figure S13).

Next, we investigated the impact of the tube material in the context of particle recovery. A highly concentrated sample of HEK293FS:CD63mNG EVs (1×10^{12} particles/ml in PBS-HAT) was diluted 100,000-fold in PBS versus PBS-HAT, stored in different tubes for 7 days and analysed by IFCM to estimate the concentration of mNG+ EVs. PBS-diluted samples were barely detectable in all containers, indicating that binding to tube surfaces was occurring in PBS for all tubes tested. However, when diluting samples in PBS-HAT buffer, the measured values resembled initial input values before dilution, indicating again that usage of PBS-HAT buffer as diluent facilitates recovery of EVs and rescues the loss of EVs due to plastic binding (Figure 14B).

These experiments clearly show how important it is to use stabilizing buffers when handling EVs, especially when diluting them before analysis. This further shows that PBS-HAT is sufficient to stabilize EV samples stored in tubes of different material even following significant sample dilution.

Lastly, to address the question how stable EVs stored in PBS-HAT would be during freeze/thaw cycles we performed IFCM analysis of mNG+ EVs for fresh samples and after up to five freeze thaw cycles. We did not observe any decline in concentration or fluorescence intensity, indicating that EVs are stable in PBS-HAT buffer even if samples are thawed and frozen over several cycles (Figure 14C).

4 | DISCUSSION

In this study, we comprehensively compared different storage strategies for cell culture derived EVs from different cell types, isolated by different EV isolation methods. With a focus on varying storage buffer composition and temperature, different EV features were assessed at different time points up to 2 years, using a variety of methods. We demonstrate that storage of EVs in PBS leads to a drastic reduction of EV recovery within days and further report that dilution of samples in PBS can severely reduce recovery even within minutes. We present several candidate buffer formulations largely preventing these observed effects and particularly identified the usage of PBS supplemented with human serum albumin and trehalose (PBS-HAT) at -80°C as overall most promising condition for sample dilutions and both short-term and long-term preservation, also throughout several freeze-thaw cycles.

The relatively broad scope and comprehensive design of this study and the inclusion of various parameters required large sample sets to be measured by various methods in relatively short timeframes to minimize time dependent effects. Thus, it was not feasible to perform independent measurements in all experiments. It is generally essential to employ a variety of methods to obtain a rather complete picture about EV stability in a certain condition and to monitor and detect potential changes in EV concentration, size, intactness, molecular cargo, surface composition, and function. Assessment of all these stability-related parameters in time-sensitive experiments is challenging and requires complementary methods, with each method having some inherent limitations. For instance, NTA would miss very small EVs and also detect non-EV particles, bulk assays such as total protein measurement provide overall insight into the abundance of molecules in a given sample volume but are not suitable to distinguish between intact and disrupted EVs or detect changes on a subpopulation level, and positive fluorescence signals obtained in cellular uptake assays do not necessarily reflect uptake of intact EVs or non-aggregated EVs. The latter point might be an explanation for the increased detection of cellular uptake for EV samples stored at 4°C compared to -20/-80°C for several buffers (Figure 5C/10C), for example. Based on such methodological limitations and the lack of independent measurements in some experiments, the authors would like to emphasize that single assay results should not generally be treated as clear evidence or be taken as basis to make ultimate conclusions. However, considering the whole picture from results derived throughout all experiments, the data clearly shows that PBS should not be used as storage buffer or as diluent for EV preparations while PBS-HAT buffer was identified as suitable EV storage buffer and diluent. The reduced recovery rates observed when using PBS were generally more severe for purer EV samples as can be seen when comparing the relative decrease of particle concentrations for EV samples prepared by TFF/UF (Stage 2) versus UC or TFF/SEC (Stage 1) and TFF/SEC (Stage 3) over time. Since PBS has been a widely used buffer for EV storage (Kusuma et al., 2018) and for diluting EV samples before analytical measurements in downstream methods such as NTA or flow cytometry, these findings are highly relevant to the EV field and for basically any experiment involving EV storage or sample dilution.

It has been reported before that EV recovery in context of EV isolation procedures can be reduced through adsorption to tube walls, SEC column surfaces or filters, and it has been shown that albumin pre-coating of the tubes or filters can prevent this, at least partially (Evtushenko et al., 2021; van de Wakker et al., 2021; Yamashita et al., 2016; Zhang et al., 2020). Here, we demonstrate that the usage of albumin-supplemented PBS as storage buffer or diluent results in clearly improved EV recovery rates compared to using PBS alone. This could be further improved when additionally adding trehalose, which was previously reported to prevent aggregation when added to PBS (Bosch et al., 2016). The observed loss of EVs of high purity in PBS and the increased recovery/stability when using PBSA/PBS-HAT buffers is supported by results from all assays performed, at all temperatures tested, and was found to be largely independent of the tube material used (Figure 14). This indicates that particularly albumin addition increases EV preservation, which appears to be at least partly due to reduced adsorption of EVs to plastic surfaces which would be saturated by albumin and thus less prone to bind EVs. Even though we observed higher recovery rates in less pure EV preparations, it ultimately remains unresolved if other proteins or additives would have similarly stabilizing effects as albumin. The extent of plastic adsorption in this context was previously estimated to account for around 2/3 of the observed losses (Evtushenko et al., 2021). However, the exact extent remains unclear due to other potentially contributing factors upstream (e.g., changing EV concentration and purity, and PBS exposure throughout isolation procedures) and downstream (e.g., dilution in PBS and exposure to plastic surfaces in instruments before measurement). There are likely other storage-related factors influencing EV stability since we observe general downtrends over time at all temperatures and in most buffers. Previous studies have also attributed loss of particles to aggregation (Bosch et al., 2016) or fusion (Gelibter et al., 2022); however, we observed no buffer-related consistent increase of particle diameters. In addition to observed quantitative differences, we included assays aiming to evaluate EV intactness and function and compared genetically engineered EVs in previously established uptake and

cytokine binding assays as well as stability of intravesicular fluorescent proteins in different buffers, over time. Again, PBS-HAT was found to be amongst the best buffers preserving these EV features.

Of note, all results presented here are based on cell culture derived EVs, and even though we include evidence that similarly beneficial effects of PBS-A/PBS-HAT buffers apply to liposomes as well, we do not claim that these results are universally applicable. It rather is recommended that – if EV samples are being stored - stability should ideally be assessed for each specific experimental context. Particularly when aiming to ultimately prepare stable batches of therapeutic EVs for clinical trials, our data after 2 years of storage highlights the importance of evaluating long-term batch stability for respective material and hopefully benefits future development of improved protocols to preserve EV-containing samples in biobanks.

There have been several reports investigating the storage stability of biofluid samples in recent years, often focusing on specific parameters such as temperature or freezing protocol, specific biofluids of interest, or investigating specific EV features such as RNA content (Barreiro et al., 2021; Cheng et al., 2019; Ge et al., 2014; Jin et al., 2016; Schulz et al., 2020; Yuana et al., 2015; Zhang et al., 2020). The stability of purified EVs in biofluid samples might differ from cell culture derived EVs depending on sample purity, EV concentration and ultimately biofluid type which likely dictates the protein corona of respective EVs which could influence their stability and plastic adsorption (Tóth et al., 2021). The EV field will surely benefit from future systematic and comprehensive comparisons of storage strategies including emerging techniques such as lyophilisation (Charoenviriyakul et al., 2018) for all types of EVs.

In conclusion, the comprehensive comparison of different storage strategies presented in this study provides relevant insight both in the context of EV sample storage and handling. We report different pitfalls related to storage and handling of EVs in non-suitable buffers and identified PBS-HAT as candidate storage buffer facilitating EV preservation for both handling and for long-term storage at -80°C. We are confident that these results are an important step towards establishing improved routines for EV preservation, ultimately for both clinical use of cell culture derived EVs and for biomarker discovery studies using EVs from biological fluids.

ACKNOWLEDGEMENTS

The authors would like to thank the electron microscopy unit at Karolinska Institutet for providing access to the electron microscope and the core facility for Bioinformatics and Expression Analysis (BEA), which is supported by the board of research at the Karolinska Institutet and the research committee at the Karolinska Hospital. Samir EL Andaloussi is supported by the Swedish Research Council (VR-Med; 4–258/2021), Evox Therapeutics, SSF-IRC (FormulaEx), H2020 (EXPERT) and ERC CoG (DELIVER; 4–628/2021). AG is an International Society for Advancement of Cytometry (ISAC) Marylou Ingram Scholar 2019–2023. Oscar P. B. Wiklander is supported by the Centre for Medical Innovation (CIMED) and KI Research grant. Helena Sork is supported by The European Regional Development Fund and the program Mobilitas Pluss (MOBJD512). Figures were partly created using BioRender.com; publication licenses can be supplied upon request.

AUTHOR CONTRIBUTIONS

André Görgens: Data curation; Formal analysis; Funding acquisition; Investigation; Methodology; Resources; Supervision; Visualization; Writing – original draft; Writing – review & editing. Giulia Corso: Conceptualization; Data curation; Formal analysis; Investigation; Methodology; Validation; Visualization; Writing – original draft; Writing – review & editing. Danie W. Hagey: Formal analysis; Investigation; Methodology; Writing – original draft; Writing – review & editing. Rim Jawad Wiklander: Investigation; Writing – original draft; Writing – review & editing. Manuela O. Gustafsson: Formal analysis; Investigation; Writing – review & editing. Ulrika Felldin: Formal analysis; Investigation; Writing – review & editing. Yi Lee: Conceptualization; Investigation; Methodology; Writing – review & editing. R. Beklem Bostancioglu: Investigation; Writing – review & editing. Helena Sork: Investigation; Methodology; Writing – review & editing. Xiuming Liang: Investigation; Writing – review & editing. Wenyi Zheng: Investigation; Writing – review & editing.Dara K. Mohammad: Formal analysis; Investigation; Methodology; Writing – review & editing.Simonides I. van de Wakker: Conceptualization; Investigation; Resources; Writing – review & editing. Pieter Vader: Investigation; Supervision; Writing – review & editing. Antje M. Zickler: Investigation; Visualization; Writing – review & editing. Doste R. Mamand: Investigation; Writing – review & editing. Li Ma: Formal analysis; Investigation; Methodology; Writing – review & editing. Margaret N. Holme: Data curation; Methodology; Supervision; Writing – review & editing. Molly M. Stevens: Resources; Supervision; Writing – review & editing. Oscar P. B. Wiklander: Conceptualization; Data curation; Formal analysis; Investigation; Methodology; Supervision; Visualization; Writing – original draft; Writing – review & editing. Samir EL Andaloussi: Conceptualization; Data curation; Formal analysis; Funding acquisition; Investigation; Methodology; Project administration; Resources; Supervision; Writing – original draft; Writing – review & editing.

DISCLOSURE STATEMENT

André Görgens, Oscar P. B. Wiklander and Samir EL Andaloussi are consultants for and have equity interests in Evox Therapeutics Ltd., Oxford, United Kingdom. André Görgens, Samir EL Andaloussi, Oscar P. B. Wiklander and Giulia Corso are inventors on the patent application 'Compositions for Extracellular Vesicle Storage and Formulation (WO2019155060). Pieter Vader serves on the scientific advisory board of Evox Therapeutics Ltd. All other authors declare no potential conflicts of interest.

ORCID

André Görgens https://orcid.org/0000-0001-9198-0857
Giulia Corso https://orcid.org/0000-0002-1145-0862
Daniel W. Hagey https://orcid.org/0000-0001-9246-6235
Rim Jawad Wiklander https://orcid.org/0000-0002-4216-0913
Manuela O. Gustafsson https://orcid.org/0000-0002-0268-9476
R. Beklem Bostancioglu https://orcid.org/0000-0001-6755-6968
Helena Sork https://orcid.org/0000-0002-5390-4420
Xiuming Liang https://orcid.org/0000-0003-0202-1211
Wenyi Zheng https://orcid.org/0000-0003-2416-5822
Dara K. Mohammad https://orcid.org/0000-0001-9201-0991
Simonides I. van de Wakker https://orcid.org/0000-0001-5480-9161
Pieter Vader https://orcid.org/0000-0002-7059-8920
Antje M. Zickler https://orcid.org/0000-0001-5001-6586
Doste R. Mamand https://orcid.org/0000-0002-4785-0796
Margaret N. Holme https://orcid.org/0000-0002-7314-9493
Molly M. Stevens https://orcid.org/0000-0002-7335-266X
Oscar P. B. Wiklander https://orcid.org/0000-0003-1176-8114

REFERENCES

Allelein, S., Medina-Perez, P., Lopes, A. L. H., Rau, S., Hause, G., Kölsch, A., & Kuhlmeier, D. (2021). Potential and challenges of specifically isolating extracellular vesicles from heterogeneous populations. *Scientific Reports*, *11*(1), 11585.

Barreiro, K., Dwivedi, O. P., Valkonen, S., Groop, P. H., Tuomi, T., Holthofer, H., Rannikko, A., Yliperttula, M., Siljander, P., Laitinen, S., Serkkola, E., Af Hallstrom, T., Forsblom, C., Groop, L., & Puhka, M. (2021). Urinary extracellular vesicles: Assessment of pre-analytical variables and development of a quality control with focus on transcriptomic biomarker research. *Journal of Extracellular Vesicles*, *10*(12), e12158.

Bosch, S., de Beaurepaire, L., Allard, M., Mosser, M., Heichette, C., Chrétien, D., Jegou, D., & Bach, J.-M. (2016). Trehalose prevents aggregation of exosomes and cryodamage. *Scientific Reports*, *6*, 36162.

Cavallaro, S., Pevere, F., Stridfeldt, F., Gorgens, A., Paba, C., Sahu, S. S., Mamand, D. R., Gupta, D., El Andaloussi, S., Linnros, J., & Dev, A. (2021). Multiparametric profiling of single nanoscale extracellular vesicles by combined atomic force and fluorescence microscopy: Correlation and heterogeneity in their molecular and biophysical features. *Small*, *17*(14), e2008155.

Charoenviriyakul, C., Takahashi, Y., Nishikawa, M., & Takakura, Y. (2018). Preservation of exosomes at room temperature using lyophilization. *International Journal of Pharmaceutics*, *553*(1-2), 1–7.

Cheng, Y., Zeng, Q., Han, Q., & Xia, W. (2019). Effect of pH, temperature and freezing-thawing on quantity changes and cellular uptake of exosomes. *Protein Cell*, *10*(4), 295–299.

Corso, G., Heusermann, W., Trojer, D., Görgens, A., Steib, E., Voshol, J., Graff, A., Genoud, C., Lee, Y., Hean, J., Nordin, J. Z., Wiklander, O. P. B., El Andaloussi, S., & Meisner-Kober, N. (2019). Systematic characterization of extracellular vesicles sorting domains and quantification at the single molecule – single vesicle level by fluorescence correlation spectroscopy and single particle imaging. *Journal of Extracellular Vesicles*, *8*(1), 1663043.

Corso, G., Mager, I., Lee, Y., Gorgens, A., Bultema, J., Giebel, B., Wood, M. J. A., Nordin, J. Z., & Andaloussi, S. E. (2017). Reproducible and scalable purification of extracellular vesicles using combined bind-elute and size exclusion chromatography. *Science Reports*, *7*(1), 11561.

Coumans, F. A. W., Brisson, A. R., Buzas, E. I., Dignat-George, F., Drees, E. E. E., El-Andaloussi, S., Emanueli, C., Gasecka, A., Hendrix, A., Hill, A. F., Lacroix, R., Lee, Y., van Leeuwen, T. G., Mackman, N., Mager, I., Nolan, J. P., van der Pol, E., Pegtel, D. M., Sahoo, S., … & Nieuwland, R. (2017). Methodological guidelines to study extracellular vesicles. *Circulation Research*, *120*(10), 1632–1648.

Dragovic, R. A., Gardiner, C., Brooks, A. S., Tannetta, D. S., Ferguson, D. J., Hole, P., Carr, B., Redman, C. W., Harris, A. L., Dobson, P. J., Harrison, P., & Sargent, I. L. (2011). Sizing and phenotyping of cellular vesicles using Nanoparticle Tracking Analysis. *Nanomedicine*, *7*(6), 780–788.

Evtushenko, E. G., Bagrov, D. V., Lazarev, V. N., Livshits, M. A., & Khomyakova, E. (2021). Adsorption of extracellular vesicles onto the tube walls during storage in solution. *PLoS One*, *15*(12), e0243738.

Ge, Q., Zhou, Y., Lu, J., Bai, Y., Xie, X., & Lu, Z. (2014). miRNA in plasma exosome is stable under different storage conditions. *Molecules (Basel, Switzerland)*, *19*(2), 1568–1575.

Gelibter, S., Marostica, G., Mandelli, A., Siciliani, S., Podini, P., Finardi, A., & Furlan, R. (2022). The impact of storage on extracellular vesicles: A systematic study. *Journal of Extracellular Vesicles*, *11*(2), e12162.

Gorgens, A., Bremer, M., Ferrer-Tur, R., Murke, F., Tertel, T., Horn, P. A., Thalmann, S., Welsh, J. A., Probst, C., Guerin, C., Boulanger, C. M., Jones, J. C., Hanenberg, H., Erdbrugger, U., Lannigan, J., Ricklefs, F. L., El-Andaloussi, S., & Giebel, B. (2019). Optimisation of imaging flow cytometry for the analysis of single extracellular vesicles by using fluorescence-tagged vesicles as biological reference material. *Journal of extracellular vesicles*, *8*(1), 1587567.

Gupta, D., Wiklander, O. P. B., Gorgens, A., Conceicao, M., Corso, G., Liang, X., Seow, Y., Balusu, S., Feldin, U., Bostancioglu, B., Jawad, R., Mamand, D. R., Lee, Y. X. F., Hean, J., Mager, I., Roberts, T. C., Gustafsson, M., Mohammad, D. K., Sork, H., … & El-Andaloussi, S. (2021). Amelioration of systemic inflammation via the display of two different decoy protein receptors on extracellular vesicles. *Nature Biomedical Engineering*, *5*(9), 1084–1098.

Gupta, D., Wiklander, O. P. B., Gorgens, A., Conceicao, M., Corso, G., Liang, X., Seow, Y., Balusu, S., Feldin, U., Bostancioglu, B., Jawad, R., Mamand, D. R., Lee, Y. X. F., Hean, J., Mager, I., Roberts, T. C., Gustafsson, M., Mohammad, D. K., Sork, H., … & El-Andaloussi, S. (2021). Amelioration of systemic inflammation via the display of two different decoy protein receptors on extracellular vesicles. *Nature Biomedical Engineering*, *5*(9), 1084–1098.

Hagey, D. W., Topcic, D., Kee, N., Reynaud, F., Bergsland, M., Perlmann, T., & Muhr, J. (2020). CYCLIN-B1/2 and -D1 act in opposition to coordinate cortical progenitor self-renewal and lineage commitment. *Nature Communications*, *11*(1), 2898.

Jeyaram, A., & Jay, S. M. (2017). Preservation and storage stability of extracellular vesicles for therapeutic applications. *The AAPS Journal*, *20*(1), 1.

Jin, Y., Chen, K., Wang, Z., Wang, Y., Liu, J., Lin, L., Shao, Y., Gao, L., Yin, H., Cui, C., Tan, Z., Liu, L., Zhao, C., Zhang, G., Jia, R., Du, L., Chen, Y., Liu, R., Xu, J., … & Wang, Y. (2016). DNA in serum extracellular vesicles is stable under different storage conditions. *BMC Cancer*, *16*(1), 753.

Koliha, N., Wiencek, Y., Heider, U., Jungst, C., Kladt, N., Krauthauser, S., Johnston, I. C., Bosio, A., Schauss, A., & Wild, S. (2016). A novel multiplex bead-based platform highlights the diversity of extracellular vesicles. *Journal of Extracellular Vesicles*, *5*, 29975.

Kusuma, G. D., Barabadi, M., Tan, J. L., Morton, D. A. V., Frith, J. E., & Lim, R. (2018). To protect and to preserve: novel preservation strategies for extracellular vesicles. *Frontiers in Pharmacology*, *9*(1199), https://doi.org/10.3389/fphar.2018.01199

Lannigan, J., & Erdbruegger, U. (2017). Imaging flow cytometry for the characterization of extracellular vesicles. *Methods (San Diego, Calif.)*, *112*, 55–67.

Lener, T., Gimona, M., Aigner, L., Borger, V., Buzas, E., Camussi, G., Chaput, N., Chatterjee, D., Court, F. A., Del Portillo, H. A., O'Driscoll, L., Fais, S., Falcon-Perez, J. M., Felderhoff-Mueser, U., Fraile, L., Gho, Y. S., Gorgens, A., Gupta, R. C., Hendrix, A., … & Giebel, B. (2015). Applying extracellular vesicles based therapeutics in clinical trials - an ISEV position paper. *Journal of Extracellular Vesicles*, *4*, 30087.

Lőrincz, Á. M., Timár, C. I., Marosvári, K. A., Veres, D. S., Otrokocsi, L., Kittel, Á., & Ligeti, E. (2014). Effect of storage on physical and functional properties of extracellular vesicles derived from neutrophilic granulocytes. *Journal of Extracellular Vesicles*, *3*, 25465–25465.

Lotvall, J., Hill, A. F., Hochberg, F., Buzas, E. I., Di Vizio, D., Gardiner, C., Gho, Y. S., Kurochkin, I. V., Mathivanan, S., Quesenberry, P., Sahoo, S., Tahara, H., Wauben, M. H., Witwer, K. W., & Thery, C. (2014). Minimal experimental requirements for definition of extracellular vesicles and their functions: A position statement from the International Society for Extracellular Vesicles. *Journal of Extracellular Vesicles*, *3*, 26913.

Maroto, R., Zhao, Y., Jamaluddin, M., Popov, V. L., Wang, H., Kalubowilage, M., Zhang, Y., Luisi, J., Sun, H., Culbertson, C. T., Bossmann, S. H., Motamedi, M., & Brasier, A. R. (2017). Effects of storage temperature on airway exosome integrity for diagnostic and functional analyses. *Journal of Extracellular Vesicles*, *6*(1), 1359478.

Mateescu, B., Kowal, E. J. K., van Balkom, B. W. M., Bartel, S., Bhattacharyya, S. N., Buzás, E. I., Buck, A. H., de Candia, P., Chow, F. W. N., Das, S., Driedonks, T. A. P., Fernández-Messina, L., Haderk, F., Hill, A. F., Jones, J. C., Van Keuren-Jensen, K. R., Lai, C. P., Lässer, C., di Liegro, I., … & Nolte-'t Hoen, E. N. M. (2017). Obstacles and opportunities in the functional analysis of extracellular vesicle RNA – An ISEV position paper. *Journal of Extracellular Vesicles*, *6*(1), 1286095.

Mihara, K., Imai, C., Coustan-Smith, E., Dome, J. S., Dominici, M., Vanin, E., & Campana, D. (2003). Development and functional characterization of human bone marrow mesenchymal cells immortalized by enforced expression of telomerase. *British Journal of Haematology*, *120*(5), 846–849.

Nordin, J. Z., Bostancioglu, R. B., Corso, G., & El Andaloussi, S. (2019). Tangential flow filtration with or without subsequent bind-elute size exclusion chromatography for purification of extracellular vesicles. *Methods in Molecular Biology*, *1953*, 287–299.

Nordin, J. Z., Lee, Y., Vader, P., Mager, I., Johansson, H. J., Heusermann, W., Wiklander, O. P., Hallbrink, M., Seow, Y., Bultema, J. J., Gilthorpe, J., Davies, T., Fairchild, P. J., Gabrielsson, S., Meisner-Kober, N. C., Lehtio, J., Smith, C. I., Wood, M. J., & El Andaloussi, S. (2015). Ultrafiltration with size-exclusion liquid chromatography for high yield isolation of extracellular vesicles preserving intact biophysical and functional properties. *Nanomedicine*, *11*(4), 879–883.

Park, S. J., Jeon, H., Yoo, S. M., & Lee, M. S. (2018). The effect of storage temperature on the biological activity of extracellular vesicles for the complement system. *In Vitro Cellular & Developmental Biology Animal*, *54*(6), 423–429.

Qin, B., Zhang, Q., Hu, X.-m., Mi, T.-y., Yu, H.-y., Liu, S.-s., Zhang, B., Tang, M., Huang, J.-f., & Xiong, K. (2020). How does temperature play a role in the storage of extracellular vesicles? *Journal of Cellular Physiology*, *235*(11), 7663–7680.

Ramirez, M. I., Amorim, M. G., Gadelha, C., Milic, I., Welsh, J. A., Freitas, V. M., Nawaz, M., Akbar, N., Couch, Y., Makin, L., Cooke, F., Vettore, A. L., Batista, P. X., Freezor, R., Pezuk, J. A., Rosa-Fernandes, L., Carreira, A. C. O., Devitt, A., Jacobs, L., … & Dias-Neto, E. (2018). Technical challenges of working with extracellular vesicles. *Nanoscale*, *10*(3), 881–906.

Resnik, M., Kovač, J., Štukelj, R., Kralj-Iglič, V., Humpolíček, P., & Junkar, I. (2020). Extracellular vesicle isolation yields increased by low-temperature gaseous plasma treatment of polypropylene tubes. *Polymers*, *12*(10), 2363.

Sahoo, S., Adamiak, M., Mathiyalagan, P., Kenneweg, F., Kafert-Kasting, S., & Thum, T. (2021). Therapeutic and diagnostic translation of extracellular vesicles in cardiovascular diseases. *Circulation*, *143*(14), 1426–1449.

Schulz, E., Karagianni, A., Koch, M., & Fuhrmann, G. (2020). Hot EVs – How temperature affects extracellular vesicles. *European Journal of Pharmaceutics and Biopharmaceutics*, *146*, 55–63.

Sokolova, V., Ludwig, A. K., Hornung, S., Rotan, O., Horn, P. A., Epple, M., & Giebel, B. (2011). Characterisation of exosomes derived from human cells by nanoparticle tracking analysis and scanning electron microscopy. *Colloids and Surfaces. B, Biointerfaces*, *87*(1), 146–150.

Tegegn, T. Z., De Paoli, S. H., Orecna, M., Elhelu, O. K., Woodle, S. A., Tarandovskiy, I. D., Ovanesov, M. V., & Simak, J. (2016). Characterization of procoagulant extracellular vesicles and platelet membrane disintegration in DMSO-cryopreserved platelets. *Journal of extracellular vesicles*, *5*, 30422.

Tertel, T., Bremer, M., Maire, C., Lamszus, K., Peine, S., Jawad, R., Andaloussi, S. E. L., Giebel, B., Ricklefs, F. L., & Gorgens, A. (2020). High-resolution imaging flow cytometry reveals impact of incubation temperature on labeling of extracellular vesicles with antibodies. *Cytometry Part A*, *97*(6), 602–609.

Thery, C., Witwer, K. W., Aikawa, E., Alcaraz, M. J., Anderson, J. D., Andriantsitohaina, R., Antoniou, A., Arab, T., Archer, F., Atkin-Smith, G. K., Ayre, D. C., Bach, J. M., Bachurski, D., Baharvand, H., Balaj, L., Baldacchino, S., Bauer, N. N., Baxter, A. A., Bebawy, M., … & Zuba-Surma, E. K. (2018). Minimal information for studies of extracellular vesicles 2018 (MISEV2018): A position statement of the International Society for Extracellular Vesicles and update of the MISEV2014 guidelines. *Journal of Extracellular Vesicles*, *7*(1), 1535750.

Tóth, E., Turiák, L., Visnovitz, T., Cserép, C., Mázló, A., Sódar, B. W., Försönits, A. I., Petővári, G., Sebestyén, A., Komlósi, Z., Drahos, L., Kittel, Á., Nagy, G., Bácsi, A., Dénes, Á., Gho, Y. S., Szabó-Taylor, K., & Buzás, E. I. (2021). Formation of a protein corona on the surface of extracellular vesicles in blood plasma. *Journal of Extracellular Vesicles*, *10*(11), e12140.

Trenkenschuh, E., Richter, M., Heinrich, E., Koch, M., Fuhrmann, G., & Friess, W. (2022). Enhancing the stabilization potential of lyophilization for extracellular vesicles. *Advanced healthcare materials*, *11*(5), 2100538.

van de Wakker, S. I., van Oudheusden, J., Mol, E. A., Roefs, M. T., Zheng, W., Görgens, A., El Andaloussi, S., Sluijter, J. P. G., & Vader, P. (2022). Influence of short term storage conditions, concentration methodsand excipients on extracellular vesicle recovery and function. *European Journal of Pharmaceutics and Biopharmaceutics*, *170*, 59–69. https://doi.org/10.1016/j.ejpb.2021.11.012

Welch, J. L., Madison, M. N., Margolick, J. B., Galvin, S., Gupta, P., Martinez-Maza, O., Dash, C., & Okeoma, C. M. (2017). Effect of prolonged freezing of semen on exosome recovery and biologic activity. *Science Reports*, *7*, 45034.

Welsh, J. A., Tang, V. A., van der Pol, E., & Gorgens, A. (2021). MIFlowCyt-EV: The next chapter in the reporting and reliability of single extracellular vesicle flow cytometry experiments. *Cytometry Part A: the journal of the International Society for Analytical Cytology*, *99*(4), 365–368.

Welsh, J. A., Van Der Pol, E., Arkesteijn, G. J. A., Bremer, M., Brisson, A., Coumans, F., Dignat-George, F., Duggan, E., Ghiran, I., Giebel, B., Gorgens, A., Hendrix, A., Lacroix, R., Lannigan, J., Libregts, S., Lozano-Andres, E., Morales-Kastresana, A., Robert, S., De Rond, L., … & Jones, J. C. (2020). MIFlowCyt-EV: A framework for standardized reporting of extracellular vesicle flow cytometry experiments. *Journal of Extracellular Vesicles*, *9*(1), 1713526.

Weng, J., Xiang, X., Ding, L., Wong, A. L.-A., Zeng, Q., Sethi, G., Wang, L., Lee, S. C., & Goh, B. C. (2021). Extracellular vesicles, the cornerstone of next-generation cancer diagnosis? *Seminars in Cancer Biology*, *74*, 105–120.

Wiklander, O. P., Nordin, J. Z., O'Loughlin, A., Gustafsson, Y., Corso, G., Mager, I., Vader, P., Lee, Y., Sork, H., Seow, Y., Heldring, N., Alvarez-Erviti, L., Smith, C. E., Le Blanc, K., Macchiarini, P., Jungebluth, P., Wood, M. J., & Andaloussi, S. E. (2015). Extracellular vesicle in vivo biodistribution is determined by cell source, route of administration and targeting. *Journal of Extracellular Vesicles*, *4*, 26316.

Wiklander, O. P. B., Bostancioglu, R. B., Welsh, J. A., Zickler, A. M., Murke, F., Corso, G., Felldin, U., Hagey, D. W., Evertsson, B., Liang, X. M., Gustafsson, M. O., Mohammad, D. K., Wiek, C., Hanenberg, H., Bremer, M., Gupta, D., Bjornstedt, M., Giebel, B., Nordin, J. Z., … & Gorgens, A. (2018). Systematic methodological evaluation of a multiplex bead-based flow cytometry assay for detection of extracellular vesicle surface signatures. *Frontiers in Immunology*, *9*(1326), 1326.

Wiklander, O. P. B., Brennan, M. Á., Lötvall, J., Breakefield, X. O., & EL Andaloussi, S. (2019). Advances in therapeutic applications of extracellular vesicles. *Science Translational Medicine*, *11*(492), eaav8521.

Willms, E., Cabañas, C., Mäger, I., Wood, M. J. A., & Vader, P. (2018). Extracellular vesicle heterogeneity: Subpopulations, isolation techniques, and diverse functions in cancer progression. *Frontiers in Immunology*, *9*, (738). https://www.frontiersin.org/article/10.3389/fimmu.2018.00738

Kenneth, W. Witwer, Edit I., Buzás, Lynne, T. Bemis, Adriana Bora, Cecilia Lässer, Jan Lötvall, Esther N, Nolte-'t, Hoen, Melissa, G., Piper, Sarada, Sivaraman, Johan Skog, Clotilde Théry, Marca H. Wauben, & Fred, Hochberg (2013). Standardization of sample collection, isolation and analysis methods in extracellular vesicle research. *Journal of Extracellular Vesicles*, 2:(1), https://doi.org/10.3402/jev.v2io.20360

Yamashita, T., Takahashi, Y., Nishikawa, M., & Takakura, Y. (2016). Effect of exosome isolation methods on physicochemical properties of exosomes and clearance of exosomes from the blood circulation. *European Journal of Pharmaceutics and Biopharmaceutics*, *98*, 1–8.

Yanez-Mo, M., Siljander, P. R., Andreu, Z., Zavec, A. B., Borras, F. E., Buzas, E. I., Buzas, K., Casal, E., Cappello, F., Carvalho, J., Colas, E., Cordeiro-da Silva, A., Fais, S., Falcon-Perez, J. M., Ghobrial, I. M., Giebel, B., Gimona, M., Graner, M., Gursel, I., … & De Wever, O. (2015). Biological properties of extracellular vesicles and their physiological functions. *Journal of Extracellular Vesicles*, *4*, 27066.

Yuan, F., Li, Y.-M., & Wang, Z. (2021). Preserving extracellular vesicles for biomedical applications: Consideration of storage stability before and after isolation. *Drug Delivery*, *28*(1), 1501–1509.

Yuana, Y., Böing, A. N., Grootemaat, A. E., van der Pol, E., Hau, C. M., Cizmar, P., Buhr, E., Sturk, A., & Nieuwland, R. (2015). Handling and storage of human body fluids for analysis of extracellular vesicles. *2015*.

Zhang, X., Borg, E. G. F., Liaci, A. M., Vos, H. R., & Stoorvogel, W. (2020). A novel three step protocol to isolate extracellular vesicles from plasma or cell culture medium with both high yield and purity. *Journal of Extracellular Vesicles*, *9*(1), 1791450.

Zhou, H., Yuen, P. S., Pisitkun, T., Gonzales, P. A., Yasuda, H., Dear, J. W., Gross, P., Knepper, M. A., & Star, R. A. (2006). Collection, storage, preservation, and normalization of human urinary exosomes for biomarker discovery. *Kidney International*, *69*(8), 1471–1476.

SUPPORTING INFORMATION

Additional supporting information can be found online in the Supporting Information section at the end of this article.

How to cite this article: Görgens, A., Corso, G., Hagey, D. W., Jawad Wiklander, R., Gustafsson, M. O., Felldin, U., Lee, Y., Bostancioglu, R. B., Sork, H., Liang, X., Zheng, W., Mohammad, D. K., van de Wakker, S. I., Vader, P., Zickler, A. M., Mamand, D. R., Ma, L., Holme, M. N., Stevens, M. M., … & EL Andaloussi, S. (2022). Identification of storage conditions stabilizing extracellular vesicles preparations. *Journal of Extracellular Vesicles*, *11,* e12238. https://doi.org/10.1002/jev2.12238